OXFORD GENETICS

GENETICS, 2021, 219(4), iyab150
DOI: 10.1093/genetics/iyab150
Advance Access Publication Date: 16 September 2021
Investigation

The sixth transmembrane region of a pheromone G-protein coupled receptor, Map3, is implicated in discrimination of closely related pheromones in *Schizosaccharomyces pombe*

Taisuke Seike [1,*,†] Natsue Sakata,[1] Chikashi Shimoda,[2] Hironori Niki,[3] and Chikara Furusawa[1,4]

[1]Center for Biosystems Dynamics Research, RIKEN, Osaka 565-0874, Japan,
[2]Department of Biology, Graduate School of Science, Osaka City University, Osaka 558-8585, Japan,
[3]Genetic Strains Research Center, National Institute of Genetics, Shizuoka 411-8540, Japan, and
[4]Universal Biology Institute, The University of Tokyo, Tokyo 113-0033, Japan

*Corresponding author: Center for Biosystems Dynamics Research, RIKEN, 6-2-3 Furuedai, Suita, Osaka 565-0874, Japan. Email: taisuke.seike@riken.jp
†Present address: Department of Bioinformatic Engineering, Graduate School of Information Science and Technology, Osaka University, 1-5 Yamadaoka, Suita, Osaka 565-0871, Japan.

Abstract

Most sexually reproducing organisms have the ability to recognize individuals of the same species. In ascomycete fungi including yeasts, mating between cells of opposite mating type depends on the molecular recognition of two peptidyl mating pheromones by their corresponding G-protein coupled receptors (GPCRs). Although such pheromone/receptor systems are likely to function in both mate choice and prezygotic isolation, very few studies have focused on the stringency of pheromone receptors. The fission yeast *Schizosaccharomyces pombe* has two mating types, Plus (P) and Minus (M). Here, we investigated the stringency of the two GPCRs, Mam2 and Map3, for their respective pheromones, P-factor and M-factor, in fission yeast. First, we switched GPCRs between *S. pombe* and the closely related species *Schizosaccharomyces octosporus*, which showed that SoMam2 (Mam2 of *S. octosporus*) is partially functional in *S. pombe*, whereas SoMap3 (Map3 of *S. octosporus*) is not interchangeable. Next, we swapped individual domains of Mam2 and Map3 with the respective domains in SoMam2 and SoMap3, which revealed differences between the receptors both in the intracellular regions that regulate the downstream signaling of pheromones and in the activation by the pheromone. In particular, we demonstrated that two amino acid residues of Map3, F214 and F215, are key residues important for discrimination of closely related M-factors. Thus, the differences in these two GPCRs might reflect the significantly distinct stringency/flexibility of their respective pheromone/receptor systems; nevertheless, species-specific pheromone recognition remains incomplete.

Keywords: yeast; *Schizosaccharomyces pombe*; pheromone; G-protein coupled receptor; discrimination

Introduction

Communication between cells is an essential feature of life. In unicellular organisms, such as yeasts, it is extremely important to find a compatible mating partner because zygote formation by cell fusion is a once-in-a-lifetime event (Johansson and Jones 2007; Fisher 1930). The specific ability of two cells of opposite mating type to recognize each other is primarily determined by molecular recognition between a mating pheromone and its cognate receptor (Bender and Sprague 1989; Gonçalves-Sá and Murray 2011; Jones and Bennett 2011; Martin *et al.* 2011). Such interactions are essential to differentiate between reproductively compatible and incompatible potential partners, and the specificity of the pheromone receptor regulates mate choice (McCullough and Herskowitz 1979; Burke *et al.* 1980; Hisatomi *et al.* 1988; Leu and Murray 2006; Gonçalves-Sá and Murray 2011; Rogers *et al.* 2015). In fact, our previous study demonstrated that genetic changes in a pheromone and its receptor genes trigger prezygotic isolation in the fission yeast *Schizosaccharomyces pombe* (Seike *et al.* 2015). Those experimental data support the idea that even a simple pheromone/receptor system has significant ability to restrict gene flow. Therefore, the specificity of pheromone recognition must be stringently maintained among individuals of the same species.

However, a recent study on the budding yeast *Saccharomyces cerevisiae* found that yeast cells do not necessarily reject mates engineered to produce pheromones from other species, even if those species had been reproductively isolated from *S. cerevisiae* (Rogers *et al.* 2015). Pheromone receptors might evolve to maximize reproductive success regardless of mate choice, potentially resulting in a relaxation of their specificity (Cardé and Baker 1984). Such evolution might also provide an opportunity to mate with a related species producing different pheromones to promote genome diversity by genetic recombination. To date, however, a few studies have investigated the stringency of pheromone receptors in yeast (Rogers *et al.* 2015; Di Roberto *et al.* 2017).

Received: August 13, 2021. **Accepted:** September 06, 2021

Most ascomycete fungi, including yeasts, produce two peptidyl mating pheromones: one is a farnesylated lipid-peptide, whereas the other is an unmodified simple peptide. *Schizosaccharomyces pombe* has two mating types, termed Plus or P-cells (h^+) and Minus or M-cells (h^-) (Gutz *et al.* 1974; Egel 1989, 2004). For *S. pombe*, M-factor, secreted by M-cells, is a lipid-peptide, and P-factor, secreted by P-cells, is a simple peptide. Notably, the distinct chemical modification states of the two pheromones are highly conserved among ascomycete fungi (Gonçalves-Sá and Murray 2011; Martin *et al.* 2011).

Pheromone receptors belong to the family of G-protein coupled receptors (GPCRs). These receptors all share a common topology of seven α-helical transmembrane (TM) helices, including three extracellular loops (ELs) and three intracellular loops (ILs), and can be classified into distinct groups at the sequence level (Vassilatis *et al.* 2003). Fungal pheromone receptors are Class D GPCRs, which form a distinct family phylogenetically distant from the well-studied rhodopsin-type (Class A) family. A study based on the primary structure of pheromone receptors of *S. cerevisiae* revealed that two types of pheromone receptor also exist in the genomes of other ascomycete fungi (Shpakov 2007; Gonçalves-Sá and Murray 2011; Martin *et al.* 2011; Wallen and Perlin 2018): one has a structure similar to that of a receptor for a lipid-peptide pheromone, whereas the other is homologous to a receptor for a simple peptide pheromone. Both the amino acid sequences and modifications of the two pheromone peptides bear no resemblance to each other.

Schizosaccharomyces pombe predominantly exists in a haploid state. Homothallic *S. pombe* strains (called h^{90}) can efficiently switch between the mating types P and M by gene transposition of the expressed mating-type locus (Miyata and Miyata 1981). On the other hand, heterothallic strains, in which mating-type switching is absent, arise from the homothallic wild type through the irreversible loss of one of the silent cassettes at the mating-type locus, resulting in the generation of the heterothallic P-strain (h^+) and M-strain (h^-). Under nitrogen-limited conditions, two haploid cells of the opposite mating type form a diploid zygote, which then undergoes meiosis followed by the formation of four haploid spores within a cell (Bresch *et al.* 1968; Egel 1971, 1989; Gutz *et al.* 1974; Nielsen 2004).

The pheromone response pathway in *S. pombe* is illustrated in Figure 1A. M-cells secrete M-factor, a farnesylated and *o*-methylated nonapeptide, which is recognized by its corresponding GPCR Map3, expressed on the surface of P-cells (Davey 1992; Tanaka *et al.* 1993). M-factor is encoded by three redundant genes, *mfm1*$^+$, *mfm2*$^+$, and *mfm3*$^+$ (Davey 1992; Kjaerulff *et al.* 1994). These genes produce precursor polypeptides of 41–44 amino acids, each of which generates a single copy of the same M-factor, YTPKVPYMC^{Far}-OCH$_3$. M-factor is actively secreted by the specific ATP-binding cassette (ABC) transporter Mam1 (Christensen *et al.* 1997). By contrast, P-cells secrete P-factor, an unmodified peptide of 23 amino acids, which activates its cognate GPCR Mam2 on the surface of M-cells (Kitamura and Shimoda 1991; Imai and Yamamoto 1994). P-factor is encoded by one gene, *map2*$^+$, and is secreted by the exocytic secretory pathway rather than by active transport (Imai and Yamamoto 1994). These pheromone signals stimulate cells of the opposite mating type to commence a mating response, and both signals are essential for mating between the two cells (Imai and Yamamoto 1994; Kjaerulff *et al.* 1994; Seike *et al.* 2013). In *S. pombe*, both the Map3 and Mam2 receptors are coupled to the monomer form of the G-protein α-subunit Gpa1 (Obara *et al.* 1991; Ladds *et al.* 2005). Activation of Gpa1 through the Map3 or Mam2 receptor transmits signals via a MAPK cascade consisting of Byr2 (MAPKKK), Byr1 (MAPKK), and Spk1 (MAPK) (Obara *et al.* 1991; Xu *et al.* 1994; Barr *et al.* 1996), thereby inducing the transcription of genes essential for mating (Mata and Bähler 2006; Xue-Franzén *et al.* 2006). In other words, the signaling pathway downstream of the activated pheromone GPCRs is the same in P- and M-cells.

The sequence homology between Map3 and Mam2 of *S. pombe* is low, a feature that is also observed between Ste3p (the receptor for the lipid-peptide pheromone a-factor) and Ste2p (the receptor for the simple peptide pheromone α-factor) of *S. cerevisiae*. Notably, sequence comparison between the pheromone receptors of *S. pombe and S. cerevisiae* shows that Map3 and Mam2 have significant sequence homology with Ste3p and Ste2p, respectively, even though these yeast species are thought to have diverged between 300 million and 1 billion years ago (Painter *et al.* 1998). For example, Mam2 of *S. pombe* and Ste2p of *S. cerevisiae* share about 70% amino acid sequence homology across the 5–7th TM helices (Lock *et al.* 2014). This observation suggests that there is an evolutionary relationship between the two subtypes of GPCRs for pheromones, Ste3p-like/Map3 and Ste2p-like/Mam2, in fungi.

We recently explored differences and similarities between genes encoding the two pheromones and their receptors in 150 wild *S. pombe* strains obtained from worldwide regions (Seike *et al.* 2019b). Sequencing analysis clearly demonstrated that there is no variation in the amino acid sequences of M-factor and Map3 in *S. pombe* strains, whereas P-factor and Mam2 show substantial diversity. Furthermore, all four P-factor variants produced by *Schizosaccharomyces octosporus* (SoP-factors) were partially recognized by Mam2 in *S. pombe* M-cells, but the single SoM-factor was not recognized by Map3 in *S. pombe* P-cells (Seike *et al.* 2019b). This implies that *S. pombe* is prezygotically isolated from *S. octosporus*, owing to a lack of compatibility of M-factor between the species. A recent study on *S. cerevisiae* reported that Ste2p, rather than Ste3p, recognizes genetically divergent pheromones (Rogers *et al.* 2015). Taken together, these observations suggest that the two GPCRs for pheromones in ascomycete fungi might have different stringencies in pheromone recognition.

Many studies on the genetic analysis of mating receptors have been conducted in *S. cerevisiae*. For example, Lorraine Marsh, a pioneer in this field, identified some mutations that improve the response to pheromones of other species by using the hybrid-species approach (Marsh 1992). Groups led by Naider *et al.* and Becker *et al.* have extensively explored the mating system of *S. cerevisiae* to describe the structure of the pheromone-binding site within the receptor and understand how the pheromone activates the signal transduction pathway through the interaction with its receptor (Kim *et al.* 2012; Uddin *et al.* 2017). Recently, several studies have focused on the evolution of ligand specificity in GPCRs (Di Roberto *et al.* 2017; Adeniran *et al.* 2018). However, the information on genetic analysis and the stringency of *S. pombe* mating receptors is scarce.

The general strategy in this study was to swap the *S. pombe* receptors, or domains thereof, with the corresponding sequences from the related species *S. octosporus*. We found that the interaction between P-factor and Mam2 seems to be relatively loose and can tolerate many variations, whereas that between M-factor and Map3 seems to be highly specific and extremely sensitive to alterations. Our domain-swapping approach revealed that the TM6 to EL3 region (residues 204–264) of Map3 is implicated in its activation by M-factor. Furthermore, by random mutagenesis of this region, we identified key residues, F214 and F215, that are important for the discrimination of closely related pheromones.

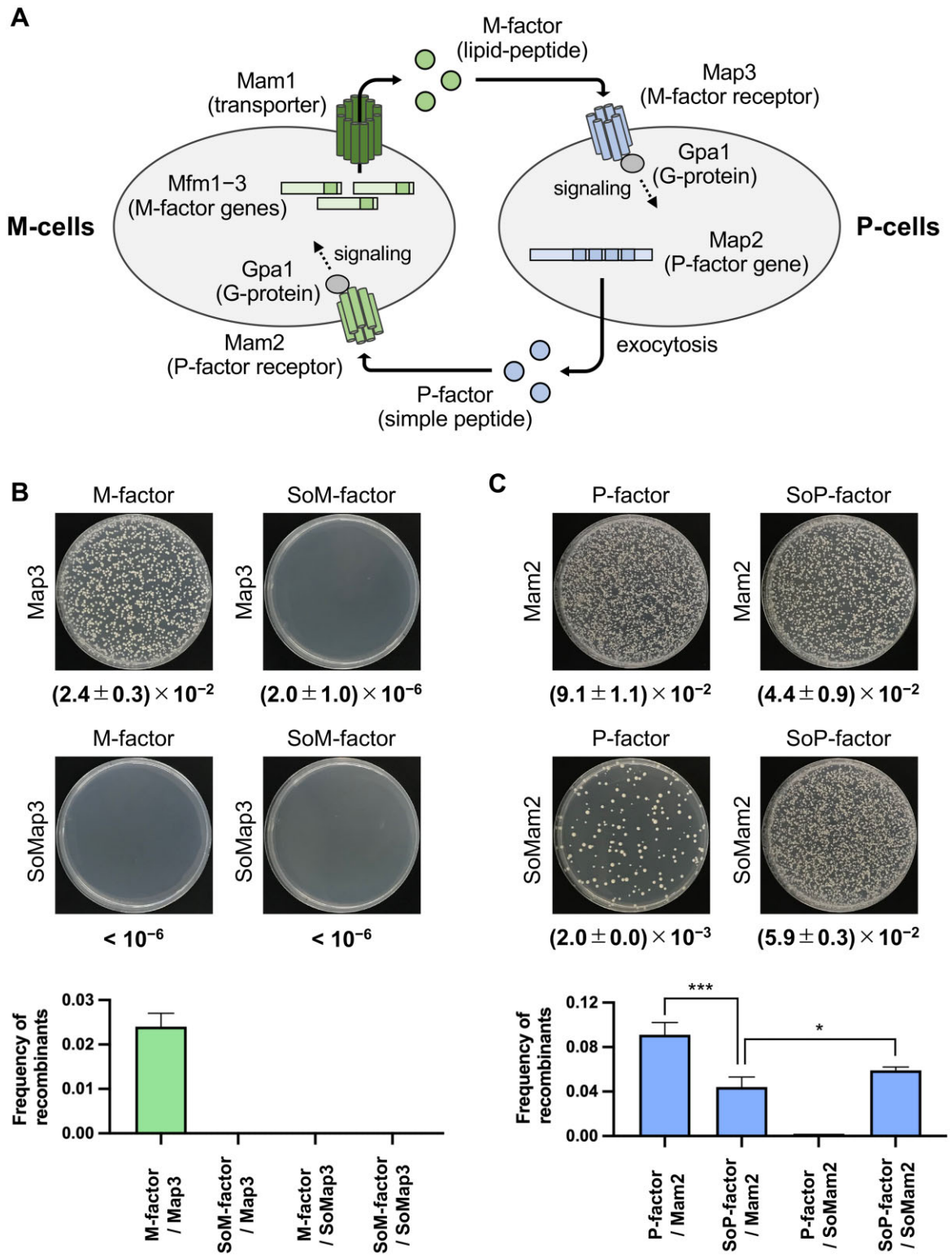

Figure 1 Recombinant frequency assay between two heterothallic *S. pombe* strains. (A) Illustration of the pheromone response pathway in *S. pombe*. M-cells produce M-factor as a lipid-peptide, which is recognized by the Map3 receptor on P-cells. The mature M-factor is encoded by the triplicate redundant *mfm1–3*$^{+}$ genes and is secreted by the Mam1 transporter. The P-cells secrete P-factor as a simple peptide, which is recognized by the Mam2 receptor on M-cells. The mature P-factor is encoded by the *map2*$^{+}$ gene and is secreted via exocytosis. The pheromone signal is transmitted through Gpa1. The signal transmission pathway is common to both M- and P-cells, and both signals are essential for mating. (B) Equal numbers of P- and M-cells were mixed and cultured on MEA medium for 2 days. The cells were then spread onto YEA medium containing 100 μg/ml of appropriate drugs. After 3 days of incubation, the plates were photographed and colony numbers were counted. The number of double-resistant colonies was normalized by the number of colonies on YEA plates without drugs. The assayed strains were TS620, M-strain secreting M-factor (kanMX6); TS9, M-strain secreting SoM-factor (kanMX6); TS26, P-strain expressing Map3 (hphMX6); and TS27, P-strain expressing SoMap3 (hphMX6). (C) The assayed strains were TS48, P-strain secreting P-factor (natMX6); TS49, P-strain secreting SoP-factor (natMX6); TS45, M-strain expressing Mam2 (hphMX6); and TS46, P-strain expressing SoMam2 (hphMX6). Each assay was performed in triplicate; and the frequency of recombinants is reported as the mean ± SD. *t*-test: $^{*}P < 0.05$; $^{***}P < 0.001$.

Our extensive study demonstrates the distinct stringencies of the Map3 and Mam2 receptors in *S. pombe*.

Materials and methods

Yeast strains, media, and culture conditions

The *S. pombe and S. octosporus* strains used in this study are listed in Supplementary Table S1. Standard methods at an incubation temperature of 30° were used for growth, mating, and sporulation (Egel and Egel-Mitani 1974; Gutz *et al.* 1974; Moreno *et al.* 1991). Yeast extract agar (YEA) medium supplemented with adenine sulfate (200 mg/ml), uracil (200 mg/ml), and L-leucine (100 mg/ml) was used for growth. Where appropriate, antibiotics (G418 disulfate [Nacalai Tesque, Kyoto, Japan], hygromycin B [Wako, Osaka, Japan], and nourseothricin ([Cosmo Bio, Tokyo, Japan]; final concentration, 100 μg/ml) were added to YEA medium. Malt extract agar (MEA) medium, synthetic sporulation liquid medium without nitrogen (SSL−N), and sporulation agar (SPA) medium were used for mating and sporulation. Synthetic dextrose (SD) medium was used to obtain auxotrophic mutants of *S. pombe*. Edinburgh minimal media (EMM2+N and EMM2−N) were used for growth in the β-galactosidase assay.

Construction of plasmids carrying various M-factor-coding genes

The plasmids and oligo-primers used in this study are listed in Supplementary Tables S2 and S3, respectively. All PCRs were performed by using KOD FX Neo DNA polymerase (TOYOBO, Tokyo, Japan). Yeast transformation was carried out using the electroporation method (Murray *et al.* 2016).

To construct pTS271, the *mfm2*$^+$ gene (~3.0 kb) containing the promoter and terminator regions was amplified from *S. pombe* (L968) genomic DNA using primer set oTS703/oTS704. Using Gibson Assembly (New England Biolabs, Ipswich, MA, USA), the DNA fragment was fused to a linearized vector derived from pFA6a-kanMX6 (Hentges *et al.* 2005), which was prepared by inverse PCR using primer set oTS35/oTS36. Next, pTS274 was constructed by inverse PCR using pTS271 and primer set oTS707/oTS708. The amplified PCR product was treated with *Dpn*I, 5′-phosphorylated by T4 polynucleotide kinase (TaKaRa, Shiga, Japan), self-ligated by T4 ligase (TaKaRa, Shiga, Japan), and then introduced into *Escherichia coli* DH5α competent cells (New England Biolabs, Ipswich, MA, USA). The resulting plasmid was integrated into a recipient *S. pombe* strain after restriction with *Afl*II near the center of the promoter region.

To construct pTS272, the *mfm3*$^+$ gene (~3.0 kb) containing promoter and terminator regions was amplified from L968 genomic DNA using primer set oTS705/oTS706. Using Gibson Assembly, the DNA fragment was fused to a linearized vector derived from pFA6a-natMX6 (Hentges *et al.* 2005), which was prepared by inverse PCR using primer set oTS35/oTS36. Next, pTS275 was constructed by inverse PCR using pTS272 and primer set oTS709/oTS710. The resulting plasmid was integrated into a recipient *S. pombe* strain after restriction with *Afe*I near the center of the promoter region.

Construction of plasmids carrying chimeric receptor genes

To construct chimeric receptor genes, we used a previously created plasmid, pFA6a-hphMX6(map3$^+$) (Seike *et al.* 2015), which we renamed pTS185 (Supplementary Table S2). To construct pTS8, the *Somap3* (*map3*$^+$ of *S. octosporus*) ORF (1092 bp) was amplified from *S. octosporus* (yFS286) genomic DNA using primer set oTS65/oTS66. Using Gibson Assembly, the DNA fragment was fused to a linearized vector derived from pTS185, which was prepared by inverse PCR using primer set oTS63/oTS64.

To construct plasmids carrying a chimeric *map3* gene, first, the corresponding region of *Somap3* was amplified by PCR using the appropriate primer set (Supplementary Table S4). Next, DNA replication using the amplified DNA fragment and pTS185 as a template was performed to generate each chimeric *map3* gene. After replication, the reaction mixture was treated with *Dpn*I to digest the template plasmid, which was transformed into DH5α. Each prepared chimeric region was confirmed by sequencing the recovered plasmid. Plasmids pTS19–pTS26, pTS42–pTS45, and pTS190–pTS199 were constructed by this method.

To replace the C-terminal region of *map3*$^+$ (nucleotides 850–1098) with the corresponding region of *Somap3*, nucleotides 844–1092 of *Somap3* were amplified from yFS286 genomic DNA using primer set oTS167/oTS168. Using Gibson Assembly, the DNA fragment was fused to a linearized vector derived from pTS185, which was prepared by inverse PCR using primer set oTS169/oTS170 to produce pTS46. Stepwise PCRs (a combination of the above) were also carried out to construct plasmids pTS91–pTS101 carrying chimeric *map3* genes in which multiple intracellular (IC) membrane regions were replaced.

To replace the C-terminal region of *Somap3* (nucleotides 844–1092) with the corresponding region of *map3*$^+$, nucleotides 850–1098 of *map3*$^+$ were amplified from L968 genomic DNA using primer set oTS63/oTS750. Using Gibson Assembly, the DNA fragment was fused to a linearized vector derived from pTS8, which was prepared by inverse PCR with primer set oTS748/oTS749 to produce pTS292. Stepwise PCRs were also carried out to construct plasmids pTS294, pTS298, and pTS299 carrying chimeric *Somap3* genes in which multiple IC membrane regions were replaced by using the appropriate primer set (Supplementary Table S4). All resulting plasmids were integrated into the genome of a recipient *S. pombe* strain after restriction with *Nru*I in the terminator region.

To construct pTS32, the *Somam2* (*mam2*$^+$ of *S. octosporus*) ORF (1047 bp) was amplified from yFS286 genomic DNA using primer set oTS128/oTS129. Using Gibson Assembly, the DNA fragment was fused to a linearized vector derived from pTS14, which was prepared by inverse PCR using primer set oTS149/oTS150. To construct plasmids carrying a chimeric *mam2* gene, inverse PCR was carried out using pTS14 and the appropriate primer set (Supplementary Table S4). The amplified PCR product was treated with *Dpn*I, 5′-phosphorylated by T4 polynucleotide kinase, self-ligated by T4 ligase, and transformed into DH5α. Each introduced mutation was confirmed by sequencing the recovered plasmid. Plasmids pTS305–pTS314 and pTS583 were constructed by this method.

To replace the C-terminal region of *Somam2* (nucleotides 904–1047) with the corresponding region of *mam2*$^+$, inverse PCR was carried out using pTS32 and primer set oTS825/oTS826 to produce pTS320. Stepwise PCRs were also carried out to construct plasmids pTS321–pTS323 carrying a chimeric *Somam2* gene in which multiple IC membrane regions were replaced by using the appropriate primer sets (Supplementary Table S4). All plasmids obtained were integrated into a recipient *S. pombe* strain after restriction with *Afe*I in the terminator region.

Construction of plasmids carrying EGFP-tagged chimeric receptor genes

To construct plasmids carrying an EGFP-tagged chimeric receptor gene, first, the EGFP fragment was amplified by PCR using the appropriate primer set (Supplementary Table S5). Next, DNA

replication using the amplified EGFP fragment and the appropriate template (Supplementary Table S5) was performed to fuse EGFP to the C-terminal end of the targeted receptor gene. To prevent internalization of the receptor by down-regulation, the C-terminal tail (*map3*$^+$, nucleotides 934–1098; *mam2*$^+$, 934–1047) was deleted as needed (Hirota *et al.* 2001). After replication, the reaction mixture was treated with *Dpn*I to digest the template plasmid, which was then transformed into DH5α. Each prepared chimeric region was confirmed by sequencing the recovered plasmid. Plasmids pTS602–pTS607, pTS610–pTS617, and pTS620–pTS622 were constructed by this method. All resulting plasmids were integrated into the genome of the recipient *S. pombe* strain after either restriction with *Nru*I in the terminator region or restriction with *Afe*I near the center of the promoter region.

Construction of plasmids carrying other pheromone signal-related genes

To construct pTS51, the *gpa1*$^+$ gene (~2.2 kb) containing promoter and terminator regions was amplified from L968 genomic DNA using primer set oTS185/oTS186. Using Gibson Assembly, the DNA fragment was fused to a linearized vector derived from pFA6a-natMX6, which was prepared by inverse PCR using primer set oTS35/oTS36. To construct pTS300, the *Sogpa1* (*gpa1*$^+$ of *S. octosporus*) ORF (1218 bp) was amplified from yFS286 genomic DNA using primer set oTS335/oTS336. Using Gibson Assembly, the DNA fragment was fused to a linearized vector derived from pTS51, which was prepared by inverse PCR using primer set oTS333/oTS334. The resulting plasmid was integrated into a recipient *S. pombe* strain after restriction with *Mfe*I near the center of the promoter region.

Construction of a *map3* mutant library

To construct plasmid pAHph-KS (named pTS302), the hphMX6 marker (~1.5 kb) containing TEF promoter and terminator regions was amplified from pFA6a-hphMX6 (Hentges *et al.* 2005) using primer set oTS797/oTS798. Using Gibson Assembly, the DNA fragment was fused to a linearized vector derived from the multicopy plasmid pAL-KS (Yazawa *et al.* 2014), which was prepared by inverse PCR using primer set oTS795/oTS796. An ~4 kb fragment containing the *map3*$^+$-coding region and promoter sequence was amplified from L968 genomic DNA using primer set oTS811/oTS812. Using Gibson Assembly, the DNA fragment was fused to a linearized pTS302 vector, which was prepared by inverse PCR using primer set oTS807/oTS808. Using the resultant plasmid (named pTS317) as a template and primer set oTS950/oTS951, nucleotides 610–792 of the *map3* ORF were subjected to random mutagenesis by using the Diversify PCR Random Mutagenesis Kit (Clontech Laboratories, Mountain View, CA, USA) in accordance with the manufacturer's instructions for error-prone PCR. To obtain a mutation rate of 5.8 mutations per 1 kb by error-prone PCR, the following reaction conditions were used: 34 µl of PCR-grade water, 5 µl of Titanium *Taq* Buffer (10×), 4 µl of $MnSO_4$ (8 mM), 3 µl of dGTP (2 mM), 1 µl of Diversify dNTP Mix (50×), 1 µl of primer mix (10 µM each), 1 µl of template DNA (1 ng/µl), and 1 µl of Titanium *Taq* Polymerase. Using Gibson Assembly, the purified PCR products were fused to a linearized vector derived from pTS317, which was prepared by inverse PCR using primer set oTS952/oTS953 to generate a mutant library comprising ~1.5×10^4 independent *E. coli* colonies (named pTS370).

Large-scale screening for *map3* mutants that suppress a mating-defective strain secreting SoM-factors

The pTS370 mutant library was transformed into homothallic strain TS400, which secretes SoM-factors. The transformants were plated on MEA medium containing hygromycin B (100 µg/ml) and colonies were inspected for diploid cells containing four spores, indicating mating ability. The colonies were subjected to iodine vapor, which turns sporulation-proficient colonies brown (Egel 1974; Seike *et al.* 2015). From a screen of ~1.2×10^5 colonies, 232 iodine-positive colonies were obtained. Microscopic inspection identified 24 colonies with asci. Plasmids were prepared from these colonies and the *map3*-coding region was sequenced by using primer set oTS157/oTS158 (see Supplementary Table S6 for the identified suppressor mutations).

To exclude the possibility that the observed suppression of mating sterility was due to an increase in copy number of relevant *map3* genes, each suppressor *map3* gene was cloned into the integration vector pFA6a. The DNA fragment containing the mutant *map3* gene was then amplified using primer set oTS124/oTS125 and fused via Gibson Assembly to a linearized vector derived from pTS185, which was prepared by inverse PCR using primer set oTS63/oTS64. These single-copy suppressor strains were examined for recovery of the sterility of M-factor mutants.

Site-directed mutagenesis of the *map3*$^+$ gene

Plasmids carrying a single amino acid substitution of *map3* were constructed by inverse PCR using pTS185 and the appropriate primer set (Supplementary Table S7). The amplified PCR product was treated with *Dpn*I, 5′-phosphorylated by T4 polynucleotide kinase, ligated by T4 ligase, and transformed into DH5α. Each introduced mutation was confirmed by sequencing the recovered plasmid. Where appropriate, stepwise inverse PCRs were performed, using the appropriate plasmid as a template, to construct plasmids carrying more than two amino acid substitutions of *map3*.

Quantitative analysis of hybrid formation by recombinant frequency

To estimate prezygotic isolation between two *S. pombe* strains, recombinant frequency was determined by a quantitative assay of genetic recombination. Heterothallic strains each carrying a chromosomal drug-resistance marker (kanMX6, hphMX6, or natMX6) were cultured on YEA medium overnight, and equal numbers of P- and M-cells were mixed in sterilized water to an OD_{600} of 5.0 (1×10^8 cells/ml). A 30-µl aliquot of the suspension was spotted onto MEA medium and incubated for 2 days at 30°. The mixed cells were allowed to mate, and the resulting hybrid diploids were subjected to sporulation. The cell suspension was serially diluted and spread on YEA medium containing different combination of antibiotics. The number of colonies was counted after 3 days of incubation at 30°. The ratio of recombinant frequency was calculated as described previously (Seike *et al.* 2013, 2015, 2019a, 2019b). Each analysis was carried out in triplicate, and the mean ± standard deviation (SD) was calculated.

Quantitation of mating frequency

Schizosaccharomyces pombe cells grown on YEA medium overnight were resuspended in sterilized water to OD_{600} of 5.0. A 30-µl aliquot of the suspension was spotted onto MEA medium and incubated for 2 days at 30°. The number of cells was counted under a differential interference contrast microscope (BX53; Olympus,

Tokyo, Japan). Cell types were classified into four groups: vegetative (non-mating) cells (V), zygotes (Z), asci (A), and free spores (S). Mating frequency was calculated by the following equation (Seike *et al.* 2012, 2013, 2015; Seike and Niki 2017; Seike *et al.* 2019a, 2019b):

$$\text{Mating (\%)} = 100 \times \{2\,(Z + A) + S/2\}/\{V + 2\,(Z + A) + S/2\}$$

In all cases, cells were counted in nine randomly photographed digital images of each strain (>1000 cells in total), and the mean ± SD was calculated (Supplementary Table S8).

RNA extraction and quantitative real-time PCR (RT-PCR)

Cells (OD_{600} of 0.1) were pre-cultured in Yeast extract (YE) liquid medium for 14 h at 30°. Cells at a density of 4×10^7 cells/ml (OD_{600} of 2.0) in 5 ml of EMM2−N were continuously shaken at 30° for 24 h (−N sample) after sampling at the start point (+N sample). Next, 1 ml of culture was harvested for RNA extraction using an RNeasy® Plus Mini Kit (Qiagen, Hilden, Germany). DNA digestion was performed to remove contaminating genomic DNA in the solution before RNA clean up. For quantitative RT-PCR, cDNA was synthesized from 100-ng samples of RNA using a PrimeScript™ RT Reagent Kit (TaKaRa, Shiga, Japan) in accordance with the manufacturer's protocol.

RT-PCR was performed by an Applied Biosystems™ StepOnePlus™ Real-Time PCR System (Thermo Fisher Scientific) using TB Green™ Premix Ex Taq™ II (TaKaRa, Shiga, Japan). The program for RT-PCR was 95° for 30 s, followed by 40 cycles of 95° for 5 s and 60° for 30 s. DNA segments containing EGFP, *map3*$^+$, *Somap3*, *mam2*$^+$, *Somam2*, and *act1*$^+$ (control) were amplified by using primer sets oTS1298/oTS1299, oTS353/oTS354, oTS1300/oTS1301, oTS355/oTS356, oTS1302/oTS1303, and oTS357/oTS358, respectively. Each analysis was carried out in triplicate, and the mean ± SD was calculated (Supplementary Table S9).

Fluorescence imaging

Cells expressing EGFP-tagged receptors were immediately analyzed by fluorescence microscopy without washing or fixation. Images were captured using cellSens standard imaging software (Olympus) and a BX53 Digital Upright Microscope (Olympus) equipped with a GFP filter, an Olympus UPlanSApo 60×/1.35 na oil objective (BX53; Olympus), and a camera (ORCA-spark; Hamamatsu).

In vitro M-factor activity assay using a *map4* promoter–*lacZ* fusion gene

Given that P-type-specific agglutinin *map4*$^+$ mRNA expression is completely dependent on M-factor signaling (Xue-Franzén *et al.* 2006) and the Map4 protein is expressed only in P-cells, expression of *map4*^{PRO}–*lacZ* was assayed by β-galactosidase activity to assess whether the chimeric receptors were activated by M-factor peptides. We used a previously created plasmid, pTA(map4-promoter: lacZ) (Seike *et al.* 2013), which we renamed pTS540 (Supplementary Table S2). First, pTS540 was introduced into a heterothallic P-type strain. For the assay, cells (OD_{600} of 0.2) were grown in EMM2+N medium lacking leucine (to avoid loss of plasmid) for 24 hours, washed with EMM2−N medium three times, and then resuspended in EMM2−N medium at a cell density of 4×10^7 cells/ml (OD_{600} of 2.0). The cells were then treated with synthetic pheromone peptide (1 μM) (Seike *et al.* 2019b) and incubated for exactly 24 hours with gentle shaking. The cell suspensions were centrifuged, and the cell pellets were resuspended in 1 ml Z-buffer (60 mM Na_2HPO_4, 40 mM NaH_2PO_4, 10 mM KCl, 1 mM $MgSO_4 \bullet 7H_2O$, and 50 mM β-mercaptoethanol, pH 7.0) and subjected to β-galactosidase assay using the sodium dodecyl sulfate (SDS)/chloroform cell permeabilization method, as previously described (Guarente 1983).

In brief, the diluted cells (OD_{600} of 1.0) were permeabilized with 5 μl of chloroform:SDS (5:4 ratio) in 150 μl of Z-buffer for 5 min at 30°, and then 30 μl of *o*-nitrophenyl-β-D-galactopyranoside (ONPG) (4 mg/ml) was added as a substrate. The cell density of the cell suspension was measured, and then the A_{420} of the cell suspension was successively determined every 5 min by a microplate reader (Infinite 200 PRO; Tecan, Männedorf, Switzerland). The background activity measured in the absence of pheromone peptides (control) was subtracted from all readings, and the normalized β-galactosidase activity was expressed as Miller units (Miller 1972). Each β-galactosidase assay was performed in triplicate, and the mean ± SD was calculated (Supplementary Table S10).

Results

Prezygotic isolation between *S. pombe* and *S. octosporus* might be due to the incompatibility of M-factor and Map3

To investigate the stringency of pheromone recognition by Map3 and Mam2, we first used genetic recombinant tests to examine whether the pheromone and receptor genes of *S. pombe* can be replaced with those of *S. octosporus*. In this test, two different drug-resistance markers were integrated into the chromosomes of heterothallic *S. pombe* strains of opposite mating type such that recombinants harboring both resistance markers would emerge if the two strains carrying different drug-resistance markers successfully mated. In other words, if no double-resistant colonies are observed, the two strains have failed to mate under this condition. This sensitive recombinant test can detect extremely rare genetic recombination events.

We constructed heterothallic *S. pombe* strains in which protein-coding sequences of their own pheromone and receptors were replaced with the corresponding coding regions of *S. octosporus* (see *Materials and methods*). Equal numbers of cells of heterothallic strains carrying different drug-resistance markers were mixed and spotted onto MEA medium to induce mating; after 2 days of incubation, an aliquot of this culture was spread onto YEA containing the appropriate drugs. The crosses between wild-type P-cells and M-cells secreting SoM-factors produced almost no double-resistant colonies (Figure 1B), consistent with our previous data showing that synthetic SoM-factors are not recognized by Map3 (Seike *et al.* 2019b). Similarly, P-cells expressing SoMap3 were completely rejected by both wild-type M-cells and M-cells secreting SoM-factors (recombinant frequency, $<10^{-6}$). By contrast, the crosses between wild-type M-cells and P-cells secreting SoP-factors generated abundant double-resistant colonies, and M-cells expressing SoMam2 were markedly accepted by both wild-type P-cells and P-cells secreting SoP-factors (Figure 1C). These data indicated that the SoP-factor and SoMam2 gene are partially effective replacements for the endogenous genes in *S. pombe*, but the assay with SoM-factor and SoMap3 resulted in failure to mate.

To exclude the possibility that SoMap3 receptors were not properly localized to the cell surface and fully expressed in *S. pombe*, we first considered analyzing the expression of EGFP-tagged receptors. In a previous study, however, the bulk of the fluorescence of Map3-GFP was internalized in the cytoplasm,

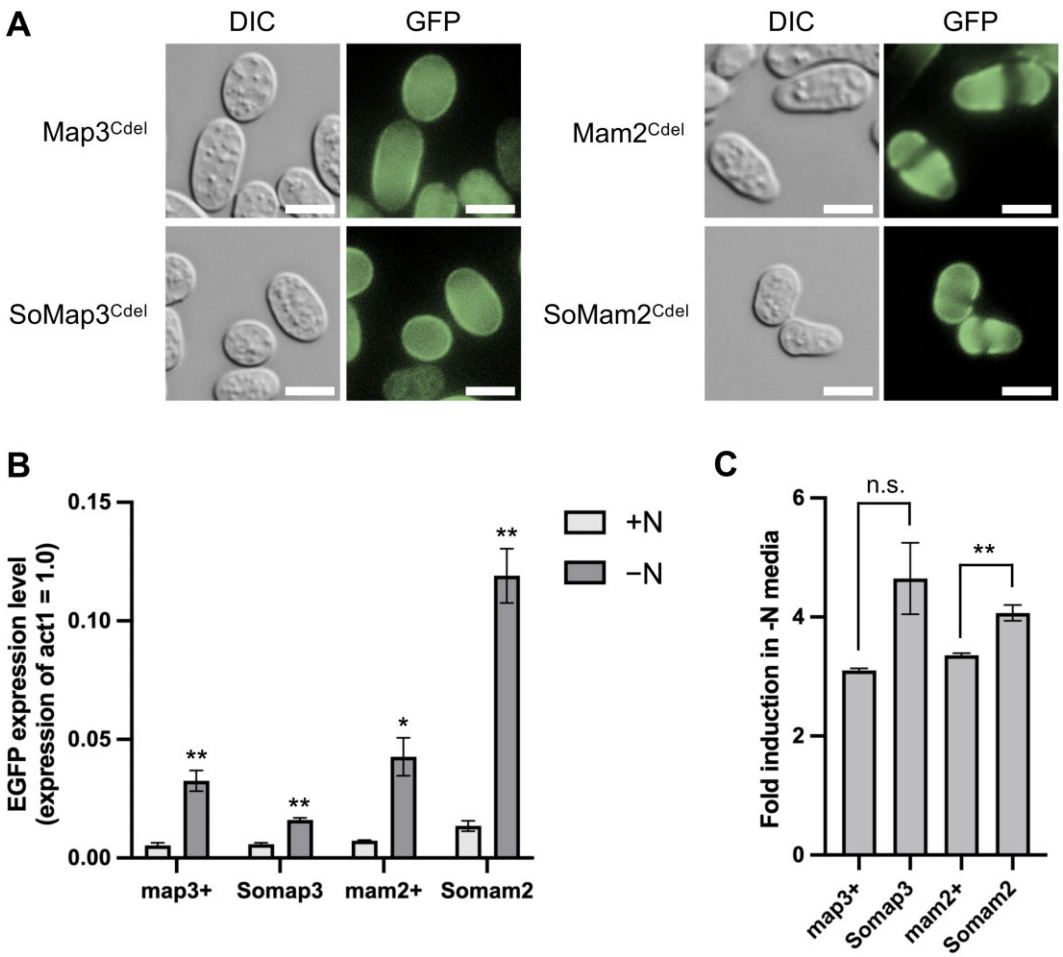

Figure 2 Localization on the cell surface and expression of SoMap3 and SoMam2 in *S. pombe*. (A) Cellular localization of Map3^{Cdel}, SoMap3^{Cdel}, Mam2^{Cdel}, and SoMam2^{Cdel} whose C-terminal tails were deleted. A homothallic strain expressing Map3^{Cdel}-EGFP (TS1234), SoMap3^{Cdel}-EGFP (TS1235), Mam2^{Cdel}-EGFP (TS1223), or SoMam2^{Cdel}-EGFP (TS1224) was grown on YEA overnight, and incubated on SPA medium for 24 hours at 30°. Cells were observed by fluorescence microscopy. All four GFP-tagged receptor proteins were localized to the cell surface. DIC, differential interference contrast; GFP, GFP filter; scale bar, 5 μm. (B) Quantitative RT-PCR showing ectopic expression of *map3*$^{+}$, *Somap3*, *mam2*$^{+}$, *Somam2* in *S. pombe* homothallic strains (TS1219, TS1220, TS1226, and TS1227). (C) Quantitative RT-PCR showing ectopic expression of *map3*$^{+}$, *Somap3*, *mam2*$^{+}$, *Somam2* in *S. pombe* heterothallic strains (TS26, TS27, TS45, and TS46). Total RNA was collected from EMM2−N cultures (0 h, +N; 24 h, −N), and RT-PCR was performed. EGFP expression was normalized by expression of *act1*$^{+}$ as a control gene. The graphs in (B) and (C) show mean ± SD. *t*-test: *$P < 0.05$; **$P < 0.01$; n.s., not significant.

leaving only a little fluorescence on the cell surface (Hirota *et al.* 2001). In this study, therefore, we constructed four receptor proteins whose C-terminal tails were deleted (written as "Cdel") and tagged them with EGFP (see *Materials and methods*). Because deletion of the C-terminal tail of the receptors is known to prevent their internalization (Bendezú and Martin 2013), the receptors should cover a large part of the cell membrane. By observing *S. pombe* homothallic strains expressing EGFP-tagged receptors during mating, we confirmed that *S. octosporus* receptors (SoMap3 and SoMam2) and *S. pombe* receptors (Map3 and Mam2) were localized to the cell surface in *S. pombe* (Figure 2A). However, these truncated receptors are not necessarily ideal for measuring the surface expression of intact receptors, and non-truncated *S. octosporus* receptors may undergo rapid internalization, possibly due to misfolding, in *S. pombe* cells.

Furthermore, we examined the transcription of the non-truncated *Somap3 and Somam2* genes in *S. pombe* homothallic strains using quantitative RT-PCR. As shown in Figure 2B, the expression level of *Somam2*-EGFP was more than twice as high as that of *mam2*-EGFP. On the other hand, the expression level of *Somap3*-EGFP was about half of that of *map3*-EGFP (Figure 2B), possibly because *map3* transcription is strengthened by M-factor signaling (Xue-Franzén *et al.* 2006). Therefore, we also examined transcription of the *Somap3 and Somam2* genes in *S. pombe* heterothallic strains (in the absence of M-factor). Figure 2C shows that the basal expression level of *S. octosporus* receptor genes induced by nitrogen starvation was the same or more than that of endogenous genes in *S. pombe*. Considering these experimental data, we determined that *Somap3 and Somam2* genes were expressed at a similar level as the *map3*$^{+}$ *and mam2*$^{+}$ genes in *S. pombe*. In addition, we showed that the *mfm1*^{So} gene was sufficiently expressed in *S. pombe* cells under nitrogen starvation (Supplementary Figure S1C). Therefore, the failure of mating between *S. pombe* transgenics of SoM-factor and SoMap3 might be due to a lack of interaction between pheromones and receptors. Thus, *S. pombe* may be prezygotically isolated from *S. octosporus*, in terms of the incompatibility between M-factor and Map3 rather than that between P-factor and Mam2.

Differences in IC regions of the receptors between two species might partially prevent G-protein signaling

Figure 3A shows the structures of Map3 and Mam2 predicted by hydropathy analysis data (Kitamura and Shimoda 1991; Tanaka *et al.* 1993). Although the amino acid sequences of Map3 and Mam2 both contain a high proportion of hydrophobic residues grouped into seven TM helices, there is no significant sequence similarity between Map3 and Mam2. The size of the proteins is similar, but Map3 and Mam2 differ markedly in the length of the N-terminal extracellular (EC) and C-terminal IC regions (Figure 3, B and C). Overall, 240 residues are identical between Map3 (365 aa) and SoMap3 (363 aa; identity, 66%; Figure 3B), and 234 residues between Mam2 (348 aa) and SoMam2 (348 aa; identity, 67%; Figure 3C). Thus, amino acid sequence homology comparison indicates that approximately two-thirds of the residues within these proteins are conserved between *S. pombe and S. octosporus*.

Due to the lack of response in the assays with SoMap3 and SoM-factor (Figure 1B), we considered the possibility that SoMap3 might not efficiently activate *S. pombe* Gpa1, which transmits downstream pheromone signaling. To test this possibility, we first generated four Map3 chimeras, in which one of the IC regions was replaced with the corresponding sequence of *S. octosporus*, by domain-swapping using PCR with the appropriate primers (see *Materials and methods*). The Map3 chimeras were then introduced into the homothallic *S. pombe map3Δ* strain secreting M-factor. We tested the mating frequency of these strains through microscopic observation. Strains expressing each of the chimeric Map3 receptors did not show a significant decrease in mating frequency as compared with wild-type Map3 (Figure 4A). Next, we carried out a stepwise replacement of the IC regions of Map3 by introducing an increasing number of *S. octosporus* IC regions into *S. pombe* Map3; results showed that the mating frequency was notably influenced by the increasing changes in Map3. Notably, the homothallic strain expressing the mutant Map3(IL1_2_3_C), in which all three ILs and the C-terminal region were replaced with the corresponding sequence of *S. octosporus*, produced less than 10% of the mating-cells of the strain expressing wild-type $map3^{+}$ (Figure 4B). Quantitative RT-PCR data showed that the mutant Map3(IL1_2_3_C) seemed to be expressed at lower levels than Map3 (Supplementary Figure S1A). We observed that the EGFP-tagged Map3(IL1_2_3_C) was internalized, resulting in reduced surface levels (Supplementary Figure S2). Thus, replacement of the IC regions of Map3 led to a lack of detectable biological activity in these assays.

We considered whether a mutant SoMap3 receptor whose IC regions were replaced with those of Map3 would be able to activate Gpa1 on interaction with SoM-factors. To examine this hypothesis, chimeric SoMap3 receptors were introduced into a homothallic *S. pombe* strain secreting SoM-factors in the presence of Gpa1 (Figure 4C). The strain expressing the mutant SoMap3(IL1_2_3_C), in which all of three ILs and the C-terminal region were replaced with the corresponding sequence of *S. pombe*, were able to mate as expected (1.3 ± 0.6%) (Figure 4D). We also observed that the EGFP-tagged SoMap3(IL1_2_3_C) accumulated mostly in the cytoplasm and only slightly at the cell surface (Supplementary Figure S2). Based on these data, we speculated that Gpa1 might be more compatible with the IC regions of Map3 than with those of SoMap3.

Next, we also found that replacement of the IC regions of SoMam2 with that of Mam2 led to an increase in mating frequency, maybe due to improved compatibility between the receptor and Gpa1 (Figure 4, E and F). In particular, the homothallic strain expressing the mutant SoMam2(IL2_3_C) showed improved mating capability with both a P-factor-secreting strain expressing the $map2^{+}$ gene (37.3 ± 3.5%) and a SoP-factor-secreting strain expressing the $map2^{So}$ gene (10.3 ± 2.2%) (Figure 4, E and F). By contrast, the strain expressing the mutant SoMam2(IL1_2_3_C), in which all the three ILs and the C-terminal region were replaced with the corresponding sequence of *S. pombe*, showed lower mating frequencies as compared with SoMam2(IL2_3_C) (Figure 4, E and F). These results suggest that the organization of the IC regions of the GPCRs might be essential for G-protein signaling (or correct folding of the receptor). In addition, a homothallic strain in which Gpa1 in a wild-type homothallic *S. pombe* strain was replaced with SoGpa1 (Gpa1 of *S. octosporus*) showed an approximately 35% reduction in mating frequency (Figure 4G). Taken together, these data imply that incompatibility between the IC regions of the two GPCRs (Map3 and Mam2) and Gpa1 may be partially responsible for interrupting pheromone signaling.

The sixth TM and third EC regions of Map3 are largely implicated in its activation by M-factor

We found that M-cells secreting SoM-factor could mate with P-cells expressing SoMap3(IL1_2_3_C) at an extremely low frequency (Figure 4D), possibly due to the whole structural changes of Map3 caused by replacing IC regions. Because the M-factor-binding site on Map3 has not been determined, we attempted to identify regions of Map3 involved in M-factor recognition. By replacing the EC and TM regions in turn with the corresponding sequences of *S. octosporus*, we generated 11 chimeric Map3 receptors. Most of the resultant homothallic strains expressing each of these chimeric receptors showed only a small decrease in mating frequency; notably, however, the replacement of TM6 and EL3 led to a complete loss of mating ability (Figure 5A), meaning that these two regions might be essential for recognition of M-factor. We also swapped the EC and TM regions of Mam2 with those of SoMam2; however, the replacement of these regions did not have a significant effect, except in the case of the N-terminal EC tail (Figure 5B). Furthermore, fluorescent observation of three chimeric EGFP-tagged receptors whose C-terminal tails were deleted showed that Map3(TM6)^{Cdel}-EGFP and Mam2-(N)^{Cdel}-EGFP were localized to the cell surface, whereas Map3(EL3)^{Cdel}-EGFP was not localized near the cell surface but was mostly accumulated in the cytoplasm (Figure 5C), suggesting that replacement of the EL3 region of Map3 might cause a defect in its folding. In addition, expression of the mutant Map3(EL3) was lower than that of Map3 (Supplementary Figure S1A). These observations may be related to differences in the molecular structures of Map3 and Mam2.

Next, we further subdivided the TM6 and EL3 regions of Map3 (residues 204–264) into eight domains (TM6-1, TM6-2, and EL3-1–EL3-6), so that each domain contained 3–4 amino acid differences between Map3 and SoMap3 (Figure 6A). Homothallic strains expressing the chimeric Map3 receptors were subjected to quantification of mating frequency with M-factor secreting cells. Notably, replacement of the TM6-2 and EL3-1 domains led to a reduction in mating frequency (Figure 6B). Based on these data, we presumed that residues critical for Map3 activation by M-factor are likely to lie within this region (residues 220–233). Therefore, we carried out site-directed mutagenesis of Map3 to create single substitutions of residues in this region (F224Y, M225L, V226L, A228V, G230C, L232G, and Q233H). Although one of these substitutions (Q233H) showed low mating frequency (4.1 ± 2.9%) (Figure 6C), none of the Map3-Q233H, Map3(TM6-2_EL3-1), and Map3(TM6_EL3) mutants recognized SoM-factor

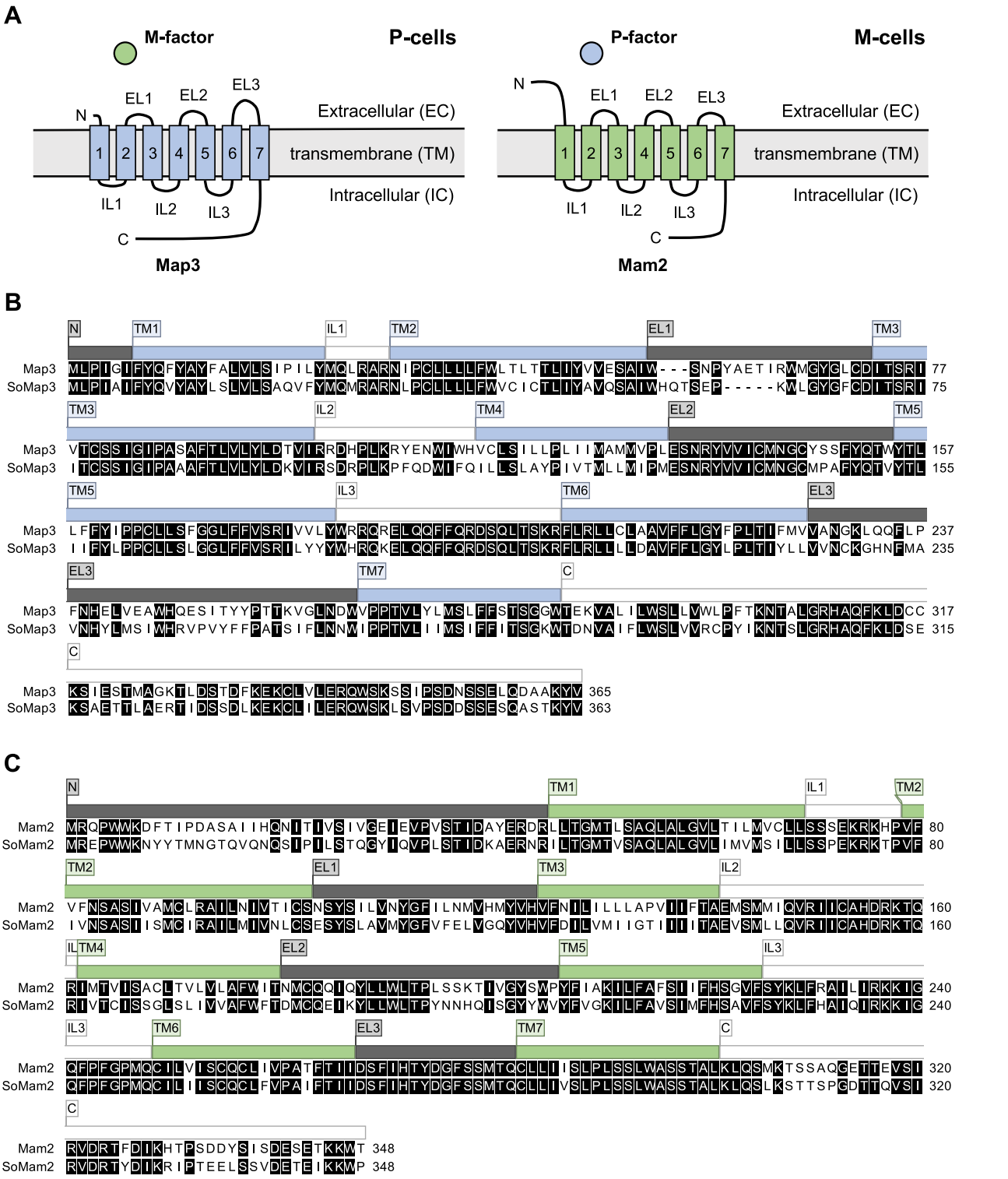

Figure 3 Comparison of the two pheromone GPCRs Map3 and Mam2. (A) Structures of Map3 (left) and Mam2 (right) predicted by hydropathy analysis. EL, extracellular loop; IL, intracellular loop; N, N-terminal tail, C, C-terminal tail. (B) Sequence alignment of the M-factor receptors Map3 (365 aa) and SoMap3 (363 aa). (C) Sequence alignment of the P-factor receptors Mam2 (348 aa) and SoMam2 (348 aa). Numerals indicate the amino acid position at the end of each line. Identical amino acids are highlighted by a white letter on a black background. Protein domains are indicated above the sequence. The alignment was generated with CLC Genomics Workbench.

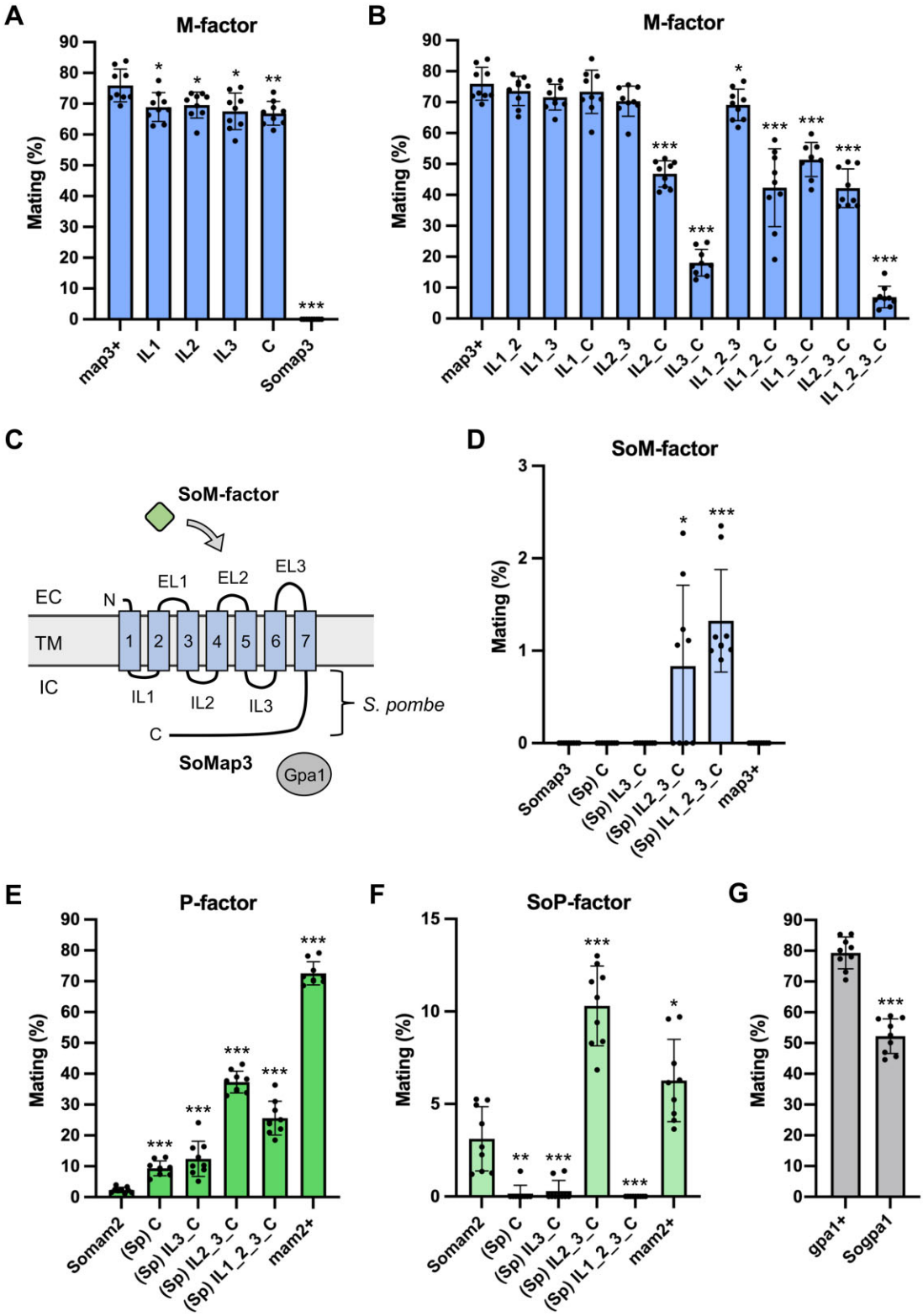

Figure 4 Genetic analysis of the intracellular regions of Map3 and Mam2 that are probably associated with Gpa1. (A) Mating frequency of homothallic M-factor-secreting strains each expressing a chimeric Map3 receptor in which one intracellular (IC) region was replaced with the corresponding sequence of *S. octosporus*. (B) Mating frequency of homothallic M-factor-secreting strains each expressing a chimeric Map3 receptor constructed by the stepwise replacement of IC regions. (C) Cartoon depicting SoM-factor signaling through SoMap3(IL1_2_3_C) and Gpa1. (D) Mating frequency of homothallic SoM-factor-secreting strains each expressing a chimeric SoMap3 in which the indicated IC regions were replaced with the corresponding sequence of *S. pombe*. (E) Mating frequency of homothallic P-factor-secreting strains each expressing a chimeric Mam2 in which one IC region was replaced with the corresponding sequence of *S. octosporus*. (F) Mating frequency of homothallic SoP-factor-secreting strains each expressing a chimeric SoMam2 in which the indicated IC regions were replaced with the corresponding sequence of *S. pombe*. (G) Mating frequency of homothallic *Sogpa1* strain. At least 1000 cells were examined for each strain. Data are the mean ± SD of nine independent samples. *t*-test: $^{*}P < 0.05$; $^{**}P < 0.01$; $^{***}P < 0.001$. EC, extracellular; TM, transmembrane; EL, extracellular loop; IL, intracellular loop; N, N-terminal tail, C, C-terminal tail.

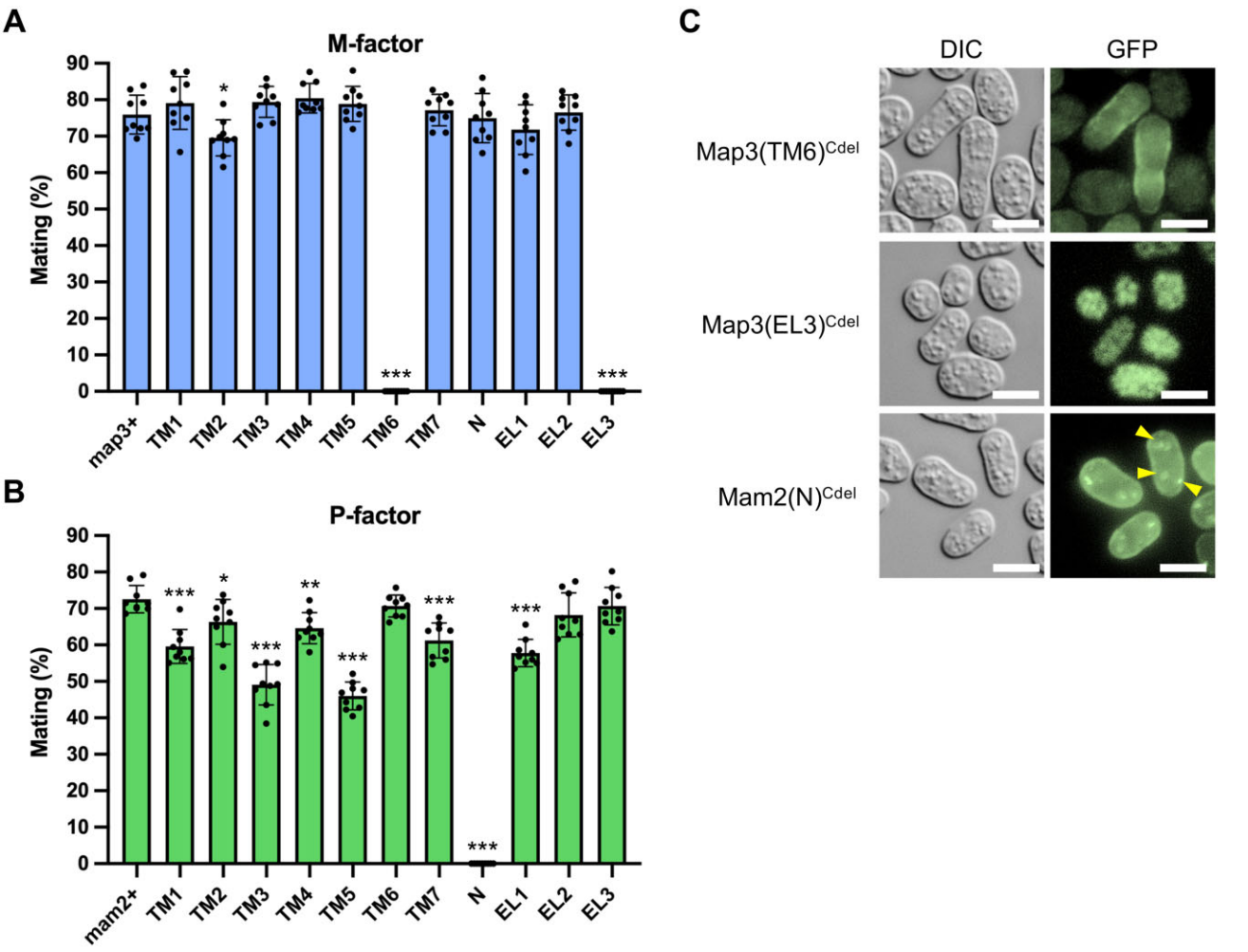

Figure 5 Genetic analysis of the extracellular regions and transmembrane regions of Map3 and Mam2. (A) Mating frequency of homothallic M-factor-secreting strains each expressing a chimeric Map3 in which one extracellular (EC) or transmembrane (TM) region was replaced with the corresponding sequence of *S. octosporus*. (B) Mating frequency of homothallic P-factor-secreting strains each expressing a chimeric Mam2 in which one EC or TM region was replaced with the corresponding sequence of *S. octosporus*. At least 1000 cells were examined for each strain. Data are the mean ± SD of nine samples. *t*-test: $^{*}P < 0.05$; $^{**}P < 0.01$; $^{***}P < 0.001$. (C) Cellular localization of Map3(TM6)^{Cdel}, Map3(EL3)^{Cdel}, and Mam2(N)^{Cdel} whose C-terminal tails were deleted. A homothallic strain expressing Map3(TM6)^{Cdel}-EGFP (TS1236), Map3(EL3)^{Cdel}-EGFP (TS1237), or Mam2(N)^{Cdel}-EGFP (TS1225) was grown on YEA overnight, and incubated on SPA medium for 24 hours at 30°. Cells were observed by fluorescence microscopy. Map3(TM6)^{Cdel}-EGFP and Mam2(N)^{Cdel}-EGFP were localized to the cell surface, but Map3(EL3)^{Cdel}-EGFP was not. Mam2(N)^{Cdel}-EGFP was partially accumulated in the cytoplasm, as indicated by arrows. DIC, differential interference contrast; GFP, GFP filter; scale bar, 5 μm.

(TS113, TS114, and TS117 failed to mate; >1000 cells in total) (Supplementary Table S1). Collectively, these data suggest that the TM6 and EL3 regions of Map3 corresponding to residues 204–264 must be important for its activation by M-factor.

Mutation of F214 and F215 in Map3 restores mating ability with *S. pombe* cells secreting SoM-factor

To find a mutant Map3 receptor that can efficiently recognize SoM-factor, we performed a random mutagenesis of the *map3* ORF (nucleotides 610–792, corresponding to residues 204–264) (Figure 6A). A high-quality *map3* mutant library constructed on a multicopy plasmid, pAHph-KS(map3^{+}) (see *Materials and methods*), was introduced into TS400, an *S. pombe* homothallic strain secreting SoM-factor. More than 10^5 colonies on MEA were inspected for mating capability using efficient colony staining with iodine vapor, as described previously (Seike *et al.* 2015). The large-scale screening yielded 232 putative mating-positive colonies, which were then microscopically inspected to eliminate false-positive colonies. Examination of mating capability identified 24 colonies in total. Plasmids were prepared from these colonies, and the nucleotide sequence of each *map3* gene was determined by Sanger sequencing, identifying 11 different mutant genes (Supplementary Table S6). Next, each of these 11 suppressor *map3* mutant genes was integrated into the *map3*$^{+}$ locus on chromosome I, and strains showing significant mating ability, even in single-copy number, were selected. Ultimately, six genuine suppressor mutations were identified (Figure 7A).

In particular, the homothallic strains expressing Map3-F215I/K231R, Map3-F214Y/F215L, or Map3-F215I showed fairly high mating frequency (37.1–58.3%; Figure 7A). In addition, the strains expressing Map3-F204S/M273V, Map3-Y95H/F204L/Q234R, or F214S/K231E/M273V showed mating, but to a small extent. We investigated whether these mutant Map3 receptors could also recognize M-factor by introducing them into the homothallic *map3*Δ strain secreting M-factor. We found that all six strains mated to some extent (Figure 7B), meaning that the mutant Map3 receptors were still able to recognize M-factor. Notably, the

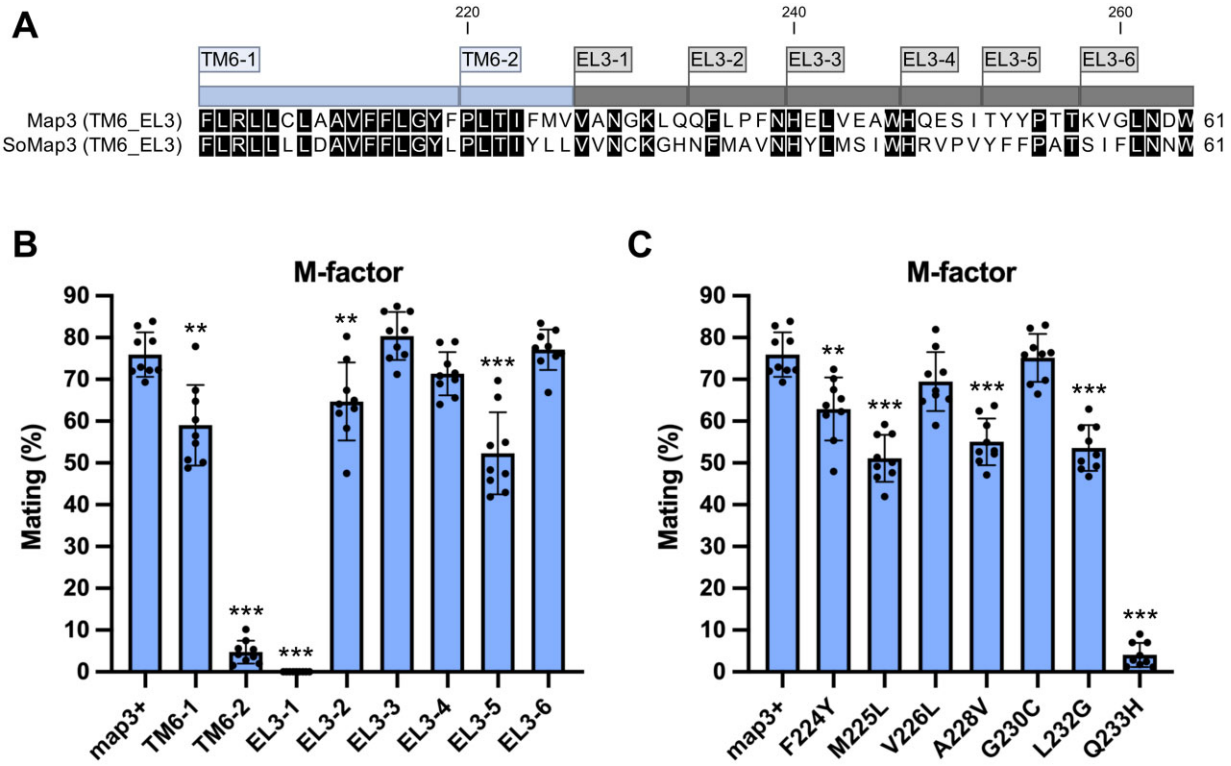

Figure 6 Genetic analysis of the region comprising residues 204–264 of Map3. (A) The 204–264-aa region of Map3 was subdivided into eight domains (TM6-1, TM6-2, and EL3-1–EL3-6), as indicated above the alignment sequence. (B) Mating frequency of homothallic M-factor-secreting strains each expressing a chimeric Map3 in which one of the eight domains was replaced. (C) Mating frequency of homothallic M-factor-secreting strains expressing Map3 with the indicated mutation. At least 1000 cells were examined for each strain. Data are the mean ± SD of nine samples. *t*-test: $^{**}P < 0.01$; $^{***}P < 0.001$.

substitution K231R of Map3 seemed to prevent the efficient recognition of M-factor [Map3-F215I (67.3 ± 3.6%) *vs* Map3-F215I/K231R (7.4 ± 2.8%); Figure 7B].

Next, we focused on the individual amino acid substitutions found in the suppressor *map3* genes and determined whether one, two, or all three substitutions were required to provide beneficial effects for SoM-factor recognition. As shown in Figure 7C, F214Y and F215I were clearly the substitutions absolutely responsible for recognizing SoM-factor. However, a mutant Map3 harboring a double substitution of F214Y and F215I did not recognize SoM-factor (Figure 7C), suggesting that these two residues, F214 and F215, in the TM6 region are independently involved in the activation by SoM-factor peptide. We also confirmed that the mutant Map3 receptors did not promote signaling in the absence of SoM-factor (TS887 and TS890 failed to mate; Supplementary Table S11), indicating that these mutant Map3s are not constitutively active receptors that function in a pheromone-independent manner.

Mutations of F214 and F215 trigger marked changes in the discrimination ability of M-factor

The six identified suppressor substitutions of Map3 seemed to have low specificity for SoM-factor, because they retained the ability to mate with a strain secreting M-factor (Figure 7B). Gola and Kothe (2003) previously called such alterations in pheromone discrimination by mutant receptors "promiscuity." We therefore attempted to search for other mating-proficient Map3 receptors that could recognize SoM-factor. Two target residues (F214 and F215) were systematically substituted to generate 38 missense *map3* mutants [19 of the F214 mutants were previously reported by our group (Seike *et al.* 2015)], in which each of the two residues was substituted with the 19 other amino acids in turn. The 38 mutated *map3* genes were each integrated at the *map3*$^{+}$ locus of two receptor-less homothallic strains secreting either M-factor or SoM-factor. The mating frequency of the 76 (38 × 2) resultant mutant strains was then inspected by determining the frequency of mating-cells (Figure 8). Microscopic observations revealed that 10 of these substitutions (F214H, F214N, F214Y, F215A, F215G, F215I, F215T, F215V, F215W, and F215Y) showed some mating proficiency (>0%) via SoM-factor from M-cells. This comprehensive mating assay indicated that some interspecific combinations of SoM-factor and mutant Map3 might be sufficiently functional even in *S. pombe*.

To confirm these mating results and the improved recognition of Map3 with SoM-factor, the activation levels of the wild-type and mutated Map3 receptors were compared *in vitro* using synthetic M-factor peptides. Map4, a P-type-specific agglutinin, is expressed in P-cells dependent on M-factor signaling. Therefore, to assess whether the mutated Map3 receptors are activated by SoM-factor peptides, we measured β-galactosidase activity under the *map4*$^{+}$ promoter (see Materials and methods). In brief, a map4^{PRO}-lacZ fusion plasmid was introduced into heterothallic P-strains, which were grown in EMM2−N medium containing synthetic peptide (M-factor or SoM-factor) at 1 μM. After permeabilization of cells, β-galactosidase activity was assayed by using ONPG as a substrate. Some of the tested Map3 receptors (>10% in Figure 8) recognized synthetic SoM-factor to a considerable extent (Table 1). As expected, two double mutants (F215I/K231R and F214Y/F215L), comprising substitutions identified from screening, gave a high level of Miller units in the presence of

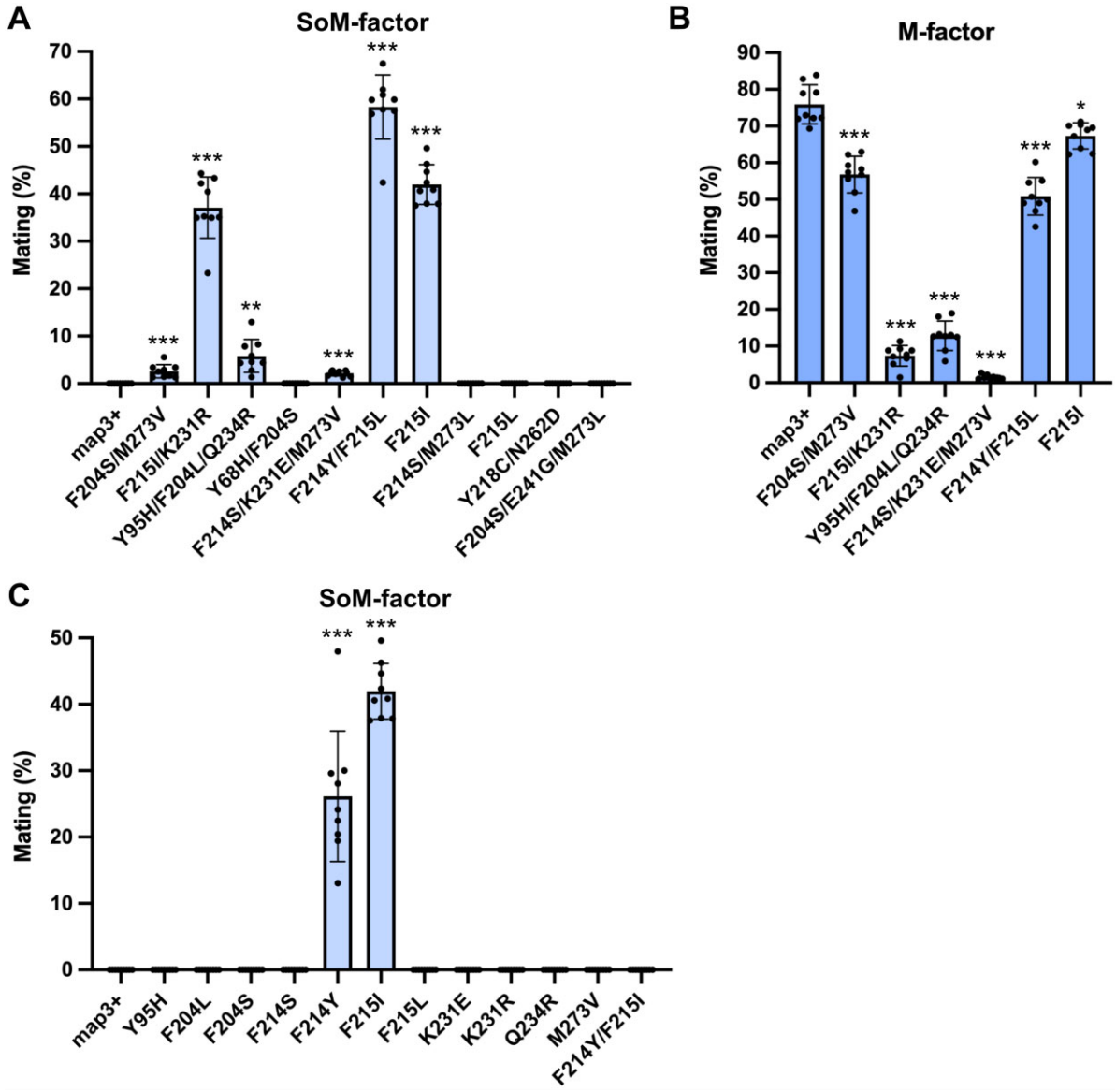

Figure 7 Identification of suppressor of Map3 that restore mating ability of homothallic SoM-factor-secreting strains. (A) Mating frequency of homothallic SoM-factor-secreting strains with one integrated copy of a suppressor *map3* gene. (B) Mating frequency of homothallic M-factor-secreting strains with one integrated copy of a suppressor *map3* gene that recognized SoM-factor. (C) Mating frequency of homothallic SoM-factor-secreting strains with one integrated copy of a *map3* gene with the indicated mutation. At least 1000 cells were examined for each strain. Data are the mean ± SD of nine samples. *t*-test: $^{*}P < 0.05$; $^{**}P < 0.01$; $^{***}P < 0.001$.

SoM-factor. We also found that the Map3-F215G showed the most efficient activation, which was approximately 13-fold higher than that of wild-type Map3. In most cases, the mutant Map3 receptors maintained the ability to be activated by M-factor, as well as SoM-factor peptides. This observation suggests that substitution of the F214 and F215 residues tends to alter the discrimination ability of Map3, enabling it to recognize both M-factor and SoM-factor. These data demonstrate that a very few mutations of the TM6 region in Map3 might facilitate cross species signaling, potentially allowing cross-reactions to occur between closely related species.

Discussion

Genetic changes of a pheromone and its receptor can affect mate choice between mating partners, providing a prezygotic barrier within a population (Rogers *et al.* 2015; Seike *et al.* 2015). In this study, we investigated the stringency of Map3 and Mam2, the two pheromone receptors of *S. pombe*. Initially, we found that SoMap3 and SoM-factor are not functional in *S. pombe* cells, whereas SoMam2 and SoP-factors partially work (Figure 1, B and C). This asymmetry in pheromone recognition is really striking: it indicates that the two GPCRs have differences in recognition of their pheromones, although they share the same downstream signaling pathway via the G-protein α-subunit Gpa1. A previous study in *S. cerevisiae* reported that the *STE3 and STE2* genes, encoding Ste3p and Ste2p respectively, are differentially regulated at both the transcriptional and the post-transcriptional level by cryptic polyadenylation (Di Segni *et al.* 2011). Thus, *S. cerevisiae* might adopt different strategies to regulate the gene expression of its two pheromone GPCRs. To our knowledge, such differences in GPCR regulation have not been reported as yet in *S. pombe* or other ascomycete fungi; however, even though the gene clusters that regulate the downstream signaling of the pheromone receptor may be similar in cells of opposite mating type, they might

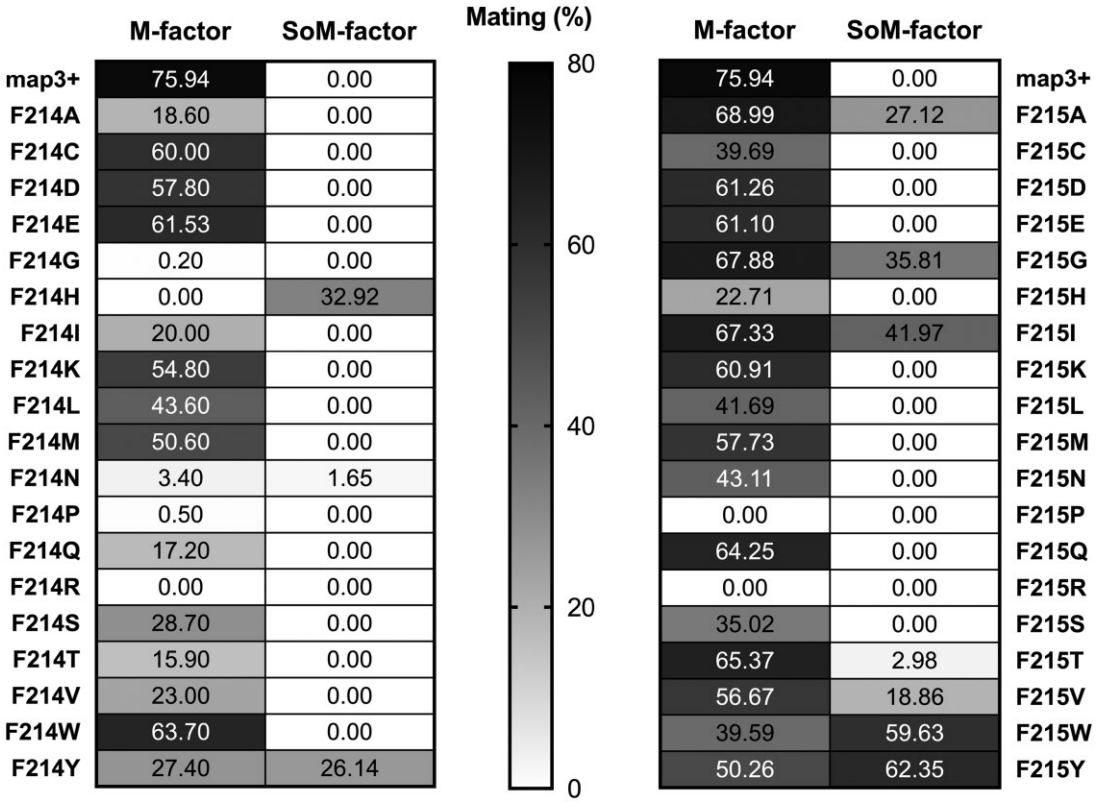

Figure 8 Mating ability of 76 *map3* missense mutants obtained after comprehensive site-directed mutagenesis of two key residues in Map3. Mating frequency of homothallic M-factor-secreting or SoM-factor-secreting strains, each expressing a missense Map3 receptor. Substitutions of the F214 and F215 residues of Map3 are indicated on the left and right. At least 1000 cells were examined for each strain. Data are the mean ± SD of nine samples. Some of the values are extracted from our study (Seike *et al.* 2015). Mating frequency is also indicated by the depth of shading, where darker shading indicates higher frequency.

Table 1 Relative activation of mutated Map3 receptors by pheromone

	Relative Miller units	
Substitution	**+M-factor (1 μM)**	**+SoM-factor (1 μM)**
map3$^+$	100	100
Somap3	35.9 ± 12.7	48.8 ± 23.4
F215I/K231R	62.2 ± 5.5	432.1 ± 19.1
F214Y/F215L	198.4 ± 28.2	515.8 ± 66.3
F214H	4.3 ± 5.0	116.6 ± 50.4
F214Y	207.5 ± 9.2	130.2 ± 11.5
F215A	609.7 ± 95.3	480.7 ± 68.0
F215G	134.9 ± 17.4	1352.5 ± 257.9
F215I	120.6 ± 9.6	88.1 ± 19.8
F215W	265.3 ± 55.5	118.7 ± 37.2
F215Y	233.9 ± 34.6	128.8 ± 26.1

Miller units are expressed as a relative value of the wild-type *map3*$^+$ gene (set at 100) after subtraction of the control value (addition of methanol instead of M-factor peptide). β-Galactosidase assays were performed in triplicate, and the mean ± SD is presented.

vary from each other in terms of characteristics such as their expression and regulation, possibly resulting in the distinct pheromone stringencies observed in yeasts.

Fungal pheromone receptors are class D GPCRs. The Mam2 receptor for P-factor contains a relatively longer N-terminal EC tail, reminiscent of Ste2p (Supplementary Figure S4). In this study, replacement of the N-terminal EC tail of Mam2 led to complete sterility (Figure 5B) and the mutant Mam2(N)^{Cdel}-EGFP was partly accumulated in the cytoplasm, in addition to localizing to the cell surface (Figure 5C); therefore, alteration of residues 1–45 might prevent the correct folding of Mam2. In addition, SoMam2 seemed to interact poorly with IC proteins of *S. pombe*, but replacement of some ILs and the C-terminal region of SoMam2 with those of Mam2 led to a great improvement in mating capability (Figure 4, E and F). Collectively, these experimental data suggest that the specificity of Mam2 for P-factors is not so stringent.

By contrast, the Map3 receptor contains a much shorter N-terminal EC tails, similar to Ste3p (Supplementary Figure S5). Although there has some research on Ste3p-like receptors in both ascomycete fungi and basidiomycete fungi, studies of the Ste3p-like GPCR are fewer than those of Ste2p-like GPCR (Hagen *et al.* 1986; Boone *et al.* 1993). In this study, systematic domain swapping of Map3 clearly showed that the TM6 and EL3 regions might be critical for M-factor recognition (Figure 5A). Previously, we introduced random mutations into the whole region of the *map3*$^+$ gene to identify suppressor mutations that restored mating in sterile M-factor mutants (Seike *et al.* 2012), and successfully identified mutations mapped to three residues: F204, F214, and E249 (Seike *et al.* 2015). Remarkably, all of these residues are located in the TM6 and EL3 regions. This observation supports the idea that the region comprising residues 204–264 is largely implicated in sensitivity to activation of M-factor. In fact, TM6 is also the location of changes that lead to several constitutively active Ste3p-like receptors (Olesnicky *et al.* 1999). However, none of the constructed chimeric receptors showed constitutively active phenotypes (TS887, TS890, and TS1191–TS1198 failed to mate; Supplementary Table S11).

The F214 residue was identified as the site of a suppressor mutation in our independent mutation studies (Supplementary

Table S6). Furthermore, our comprehensive mating assay showed that two consecutive phenylalanine residues, F214 and F215, affect recognition of M-factor peptide, with significant differences between the two residues. For example, F215 seemed to show a more gradually reduced specificity for M-factor as compared with F214 (Figure 8). In the *in vitro* activity assay for M-factor, some of the mutant Map3 receptors in which F215 was substituted were activated by SoM-factor at an unexpectedly high level (Table 1), suggesting that this substitution relaxes the specificity of Map3. We demonstrated that *S. pombe* P-cells expressing any of the single-mutant Map3 receptors (F214H, F214Y, F215A, F215G, F215I, F215W, and F215Y) were able to mate with *S. pombe* M-cells secreting SoM-factor (*i.e.*, without wild-type M-factor or Map3) (Figure 8). These two residues, F214 and F215, are conserved among the genus *Schizosaccharomyces* (Supplementary Figure S5), but their mutation may disturb mate choice (similar to promiscuity), potentially allowing *S. pombe* cells to form a diploid zygote by crossing with different species. Amino acid residues located in the TM6 helix are highly conserved, whereas the EL3 region is largely varied among species (Supplementary Figure S5). In this regard, we note that Q233 in the EL3, which affected mating efficiency (Figure 6C), is replaced by His (basic amino acid) in both *S. octosporus and Schizosaccharomyces cryophilus* and by Glu (acidic amino acid) in *Schizosaccharomyces japonicus* (Supplementary Figure S5). Thus, the EL3 region may be one of the important regions for facilitating structural changes of Map3.

None of the loss-of-function mutant receptors that we constructed in this study showed dramatic dominant-negative activity (Supplementary Figure S3). The *S. pombe* strain coexpressing Mam2 and SoMam2 showed a reduction of about 20% in mating frequency (Supplementary Figure S3B), but this was possibly because Mam2 form a dimer (Velazhahan *et al.* 2021). Further experiments are necessary to understand in detail the molecular recognition of pheromone peptides by GPCRs and the specificity of both the interaction between a pheromone and its receptor and between the receptor and downstream IC proteins. However, we have clearly demonstrated that the stringencies of the Class D GPCRs Map3 and Mam2 differ significantly based on mating and recombinant assays using *S. pombe* strains expressing various chimeric receptor genes and pheromones. This difference is likely to be linked to the asymmetric diversification of M-factor and P-factor in nature (Seike *et al.* 2019b). Why would such an asymmetric setting be beneficial for yeast life? Although we have no explanations or working hypotheses for this finding at present, in future studies we plan to conduct simulation modeling of the evolutionary process to understand the effects of fixing pheromone communication in one direction. Fungal pheromone receptors might be the result of convergent evolution, shedding light on the pheromone signaling pathway and the functions of these uncharacterized GPCRs. Our study also showed that the TM6 and EL3 regions of Map3 are largely implicated in mate choice between *S. pombe and S. octosporus*. This finding might serve as a starting point for further mutagenesis studies to elucidate the structure–function relationship of the Class D GPCRs, as well as the molecular mechanism of prezygotic isolation caused by genetic changes of a pheromone/receptor system.

Data availability

All relevant data are included in the paper and its Supplemental Material.

Supplementary material is available at *GENETICS* online.

Acknowledgments

We thank the National Bio-Resource Project (NBRP), Japan, for providing yeast strains and plasmids. We are also sincerely grateful to Dr. Taro Nakamura of Osaka City University for helpful comments and all members of our laboratory for beneficial suggestions.

Author contributions

Conceptualization: T.S., C.S., and H.N. Data curation: T.S. and N.S. Formal analysis: T.S. and N.S. Funding acquisition: T.S. Supervision: C.F. Writing—original draft: T.S. Writing—review and editing: C.S., H.N., and C.F.

Funding

This study was supported by Japan Society for the Promotion of Science KAKENHI https://kaken.nii.ac.jp/en/index/ (grant number JP11J02671, JP15J03416, JP17K15181, JP19K16197, and JP20H04790) to T.S. The funders had no role in study design, data collection and analysis, decision to publish, or preparation of the manuscript.

Conflicts of interest

The authors have declared that no competing interests exist.

Literature cited

Adeniran A, Stainbrook S, Bostick JW, Tyo KEJ. 2018. Detection of a peptide biomarker by engineered yeast receptors. ACS Synth Biol. 7:696–705. doi:10.1021/acssynbio.7b00410.

Barr MM, Tu H, Van Aelst L, Wigler M. 1996. Identification of Ste4 as a potential regulator of Byr2 in the sexual response pathway of *Schizosaccharomyces pombe*. Mol Cell Biol. 16:5597–5603. doi:10.1128/mcb.16.10.5597.

Bender A, Sprague GF. 1989. Pheromones and pheromone receptors are the primary determinants of mating specificity in the yeast *Saccharomyces cerevisiae*. Genetics. 121:463–476.

Bendezú FO, Martin SG. 2013. Cdc42 explores the cell periphery for mate selection in fission yeast. Curr Biol. 23:42–47. doi:10.1016/j.cub.2012.10.042.

Boone C, Davis NG, Sprague GF. 1993. Mutations that alter the third cytoplasmic loop of the a-factor receptor lead to a constitutive and hypersensitive phenotype. Proc Natl Acad Sci U S A. 90:9921–9925. doi:10.1073/pnas.90.21.9921.

Bresch C, Müller G, Egel R. 1968. Genes involved in meiosis and sporulation of a yeast. Mol Gen Genet. 102:301–306. doi:10.1007/BF00433721.

Burke D, Mendonca-Previato L, Ballou CE. 1980. Cell-cell recognition in yeast: purification of *Hansenula wingei* 21-cell sexual agglutination factor and comparison of the factors from three genera. Proc Natl Acad Sci U S A. 77:318–322. doi:10.1073/pnas.77.1.318.

Cardé RT, Baker TC. 1984. Sexual communication with pheromones. In: Bell WJ and Cardé RT, editors. Chemical Ecology of Insects. Boston, MA: Springer. p. 355–383.

Christensen PU, Davey J, Nielsen O. 1997. The *Schizosaccharomyces pombe* mam1 gene encodes an ABC transporter mediating secretion of M-factor. Mol Gen Genet. 255:226–236. doi:10.1007/s004380050493.

Davey J. 1992. Mating pheromones of the fission yeast *Schizosaccharomyces pombe*: purification and structural characterization of M-factor and isolation and analysis of two genes encoding the pheromone. Embo J. doi:10.1002/j.1460-2075.1992.tb05134.x.

Di Segni G, Gastaldi S, Zamboni M, Tocchini-Valentini GP. 2011. Yeast pheromone receptor genes STE2 and STE3 are differently regulated at the transcription and polyadenylation level. Proc Natl Acad Sci USA. 108:17082–17086.

Egel R. 1971. Physiological aspects of conjugation in fission yeast. Planta. 98:89–96. doi:10.1007/BF00387025.

Egel R. 1974. Fission yeast in general genetics. In: R Egel, editor. The Molecular Biology of Schizosaccharomyces pombe. Berlin/Heidelberg: Springer. p. 1–12.

Egel R. 1989. Mating-type genes, meiosis, and sporulation. In: A Nasim, P Young, BF, editors. Johnson Molecular Biology of the Fission Yeast. San Diego, CA: Academic Press. p. 31–73.

Egel R. 2004. Fission yeast in general genetics. In: R Egel, editor. The Molecular Biology of Schizosaccharomyces pombe. Berlin: Springer. p. 1–12.

Egel R, Egel-Mitani M. 1974. Premeiotic DNA synthesis in fission yeast. Exp Cell Res. 88:127–134. doi:10.1016/0014-4827(74)90626-0.

Fisher RA. 1930. The Genetical Theory of Natural Selection. London, UK: Oxford University Press.

Gola S, Kothe E. 2003. The little difference: in vivo analysis of pheromone discrimination in Schizophyllum commune. Curr Genet. 42:276–283.

Gonçalves-Sá J, Murray A. 2011. Asymmetry in sexual pheromones is not required for ascomycete mating. Curr Biol. 21:1337–1346. doi: 10.1016/j.cub.2011.06.054.

Guarente L. 1983. Yeast promoters and lacZ fusions designed to study expression of cloned genes in yeast. Methods Enzymol. 101: 181–191. doi:10.1016/0076-6879(83)01013-7.

Gutz H, Heslot U, Leupold LN. 1974. Handbook of Genetics. New York: Plenum Press.

Hagen DC, McCaffrey G, Sprague GF. 1986. Evidence the yeast STE3 gene encodes a receptor for the peptide pheromone a factor: gene sequence and implications for the structure of the presumed receptor. Proc Natl Acad Sci U S A. 83:1418–1422. doi: 10.1073/pnas.83.5.1418.

Hentges P, Van Driessche B, Tafforeau L, Vandenhaute J, Carr AM. 2005. Three novel antibiotic marker cassettes for gene disruption and marker switching in *Schizosaccharomyces pombe*. Yeast. 22: 1013–1019. doi:10.1002/yea.1291.

Hirota K, Tanaka K, Watanabe Y, Yamamoto M. 2001. Functional analysis of the C-terminal cytoplasmic region of the M-factor receptor in fission yeast. Genes Cells. 6:201–214. doi:10.1046/j.1365-2443.2001.00415.x.

Hisatomi T, Yanagishima N, Sakurai A, Kobayashi H. 1988. Interspecific actions of α mating pheromones on the *a* mating-type cells of three Saccharomyces yeasts. Curr Genet. 13: 25–27.

Imai Y, Yamamoto M. 1994. The fission yeast mating pheromone P-factor: its molecular structure, gene structure, and ability to induce gene expression and G1 arrest in the mating partner. Genes Dev. 8:328–338. doi:10.1101/gad.8.3.328.

Johansson BG, Jones TM. 2007. The role of chemical communication in mate choice. Biol Rev. 82:265–289.

Jones SK, Bennett RJ. 2011. Fungal mating pheromones: choreographing the dating game. Fungal Genet Biol. 48:668–676.

Kim K-M, Lee Y-H, Akal-Strader A, Uddin MS, Hauser M, *et al.* 2012. Multiple regulatory roles of the carboxy terminus of Ste2p a yeast GPCR. Pharmacol Res. 65:31–40. doi: 10.1016/j.phrs.2011.11.002.Multiple.

Kitamura K, Shimoda C. 1991. The *Schizosaccharomyces pombe* mam2 gene encodes a putative pheromone receptor which has a significant homology with the *Saccharomyces cerevisiae* Ste2 protein. EMBO J. 10:3743–3751.

Kjaerulff S, Davey J, Nielsen O. 1994. Analysis of the structural genes encoding M-factor in the fission yeast *Schizosaccharomyces pombe*: identification of a third gene, mfm3. Mol Cell Biol. 14:3895–3905. doi:10.1128/mcb.14.6.3895.

Ladds G, Davis K, Das A, Davey J. 2005. A constitutively active GPCR retains its G protein specificity and the ability to form dimers. Mol Microbiol. 55:482–497.

Leu JY, Murray AW. 2006. Experimental evolution of mating discrimination in budding yeast. Curr Biol. 16:280–286.

Lock A, Forfar R, Weston C, Bowsher L, Uptond GJG, *et al.* 2014. One motif to bind them: a small-XXX-small motif affects transmembrane domain 1 oligomerization, function, localization, and cross-talk between two yeast GPCRs. Biochim Biophys Acta Biomembr.1838:3036–3051.

Marsh L. 1992. Substitutions in the hydrophobic core of the alpha-factor receptor of *Saccharomyces cerevisiae* permit response to *Saccharomyces kluyveri* alpha-factor and to antagonist. Mol Cell Biol. 12:3959–3966. doi:10.1128/mcb.12.9.3959-3966.1992.

Martin SH, Wingfield BD, Wingfield MJ, Steenkamp ET. 2011. Causes and consequences of variability in peptide mating pheromones of ascomycete fungi. Mol Biol Evol. 28:1987–2003. doi: 10.1093/molbev/msr022.

Mata J, Bähler J. 2006. Global roles of Ste11p, cell type, and pheromone in the control of gene expression during early sexual differentiation in fission yeast. Proc Natl Acad Sci U S A. 103: 15517–15522. doi:10.1073/pnas.0603403103.

McCullough J, Herskowitz I. 1979. Mating pheromones of *Saccharomyces kluyveri*: pheromone interactions between *Saccharomyces kluyveri* and *Saccharomyces cerevisiae*. J Bacteriol. 138:146–154. doi:10.1128/jb.138.1.146-154.1979.

Miller J. 1972. Experiments in Molecular Biology. Cold Spring Harbor, NY: Cold Spring Harbor Laboratory Press.

Miyata H, Miyata M. 1981. Mode of conjugation in homothallic cells of *Schizosaccharomyces pombe*. J Gen Appl Microbiol. 27:365–371. doi:10.2323/jgam.27.365.

Moreno S, Klar A, Nurse P. 1991. Molecular genetic analysis of fission yeast *Schizosaccharomyces pombe*. Methods Enzymol. 194:795–823. doi:10.1016/0076-6879(91)94059-L.

Murray JM, Watson AT, Carr AM. 2016. Transformation of *Schizosaccharomyces pombe*: electroporation procedure. Cold Spring Harb Protoc. 2016:pdb.prot090951.doi:10.1101/pdb.prot090951.

Nielsen O. 2004. Mating-type control and differentiation. In: The Molecular Biology of Schizosaccharomyces pombe.

Obara T, Nakafuku M, Yamamoto M, Kaziro Y. 1991. Isolation and characterization of a gene encoding a G-protein alpha subunit from *Schizosaccharomyces pombe*: involvement in mating and sporulation pathways. Proc Natl Acad Sci U S A. 88:5877–5881. doi: 10.1073/pnas.88.13.5877.

Olesnicky NS, Brown AJ, Dowell SJ, Casselton LA. 1999. A constitutively active G-protein-coupled receptor causes mating self-compatibility in the mushroom Coprinus. EMBO J. 18: 2756–2763. doi:10.1093/emboj/18.10.2756.

Painter RB, Nickoloff JA, Hoekstra MF. 1998. DNA damage and repair, volume I: DNA repair in prokaryotes and lower eukaryotes. Radiat Res. 149:654–655.

Roberto RB, Di B, Chang SG., Peisajovich 2017. The directed evolution of ligand specificity in a GPCR and the unequal contributions of efficacy and affinity. Sci Rep. 7:1–11. doi:10.1038/s41598-017-16332-2.

Rogers DW, Denton JA, McConnell E, Greig D. 2015. Experimental evolution of species recognition. Curr Biol. 25:1753–1758. doi: 10.1016/j.cub.2015.05.023.

Seike T, Maekawa H, Nakamura T, Shimoda C. 2019a. The asymmetric chemical structures of two mating pheromones reflect their

differential roles in mating of fission yeast. J Cell Sci. 132: doi: 10.1242/jcs.230722.
Seike T, Nakamura T, Shimoda C. 2013. Distal and proximal actions of peptide pheromone M-factor control different conjugation steps in fission yeast. PLoS One. 8:e69491.doi:10.1371/journal.-pone.0069491.
Seike T, Nakamura T, Shimoda C. 2015. Molecular coevolution of a sex pheromone and its receptor triggers reproductive isolation in *Schizosaccharomyces pombe*. Proc Natl Acad Sci U S A. 112: 4405–4410. doi:10.1073/pnas.1501661112.
Seike T, Niki H. 2017. Mating response and construction of heterothallic strains of the fission yeast *Schizosaccharomyces octosporus*. FEMS Yeast Res. 17:1–14. doi:10.1093/femsyr/fox045.
Seike T, Shimoda C, Niki H. 2019b. Asymmetric diversification of mating pheromones in fission yeast. PLoS Biol. 17:e3000101.doi: 10.1371/journal.pbio.3000101.
Seike T, Yamagishi Y, Iio H, Nakamura T, Shimoda C. 2012. Remarkably simple sequence requirement of the M-factor pheromone of *Schizosaccharomyces pombe*. Genetics. 191:815–825. doi: 10.1534/genetics.112.140483.
Shpakov AO. 2007. Serpentine type receptors and heterotrimeric G-proteins in yeasts: structural-functional organization and molecular mechanisms of action. J Evol Biochem Physiol. 43:1–25.
Tanaka K, Davey J, Imai Y, Yamamoto M. 1993. *Schizosaccharomyces pombe* map3+ encodes the putative M-factor receptor. Mol Cell Biol. 13:80–88. doi:10.1128/mcb.13.1.80.
Uddin MS, Naider F, Becker JM. 2017. Dynamic roles for the N-terminus of the yeast G protein-coupled receptor Ste2p. Biochim Biophys Acta Biomembr. 1859:2058–2067. doi:10.1016/j.bbamem.2017.07.014.
Vassilatis DK, Hohmann JG, Zeng H, Li F, Ranchalis JE, *et al.* 2003. The G protein-coupled receptor repertoires of human and mouse. Proc Natl Acad Sci U S A. 100:4903–4908.
Velazhahan V, Ma N, Pándy-Szekeres G, Kooistra AJ, Lee Y, *et al.* 2021. Structure of the class D GPCR Ste2 dimer coupled to two G proteins. Nature. 589:148–153. doi:10.1038/s41586-020-2994-1.
Wallen RM, Perlin MH. 2018. An overview of the function and maintenance of sexual reproduction in dikaryotic fungi. Front Microbiol. 9:503–524. doi:10.3389/fmicb.2018.00503.
Xu HP, White M, Marcus S, Wigler M. 1994. Concerted action of RAS and G proteins in the sexual response pathways of *Schizosaccharomyces pombe*. Mol Cell Biol. 14:50–58. doi:10.1128/mcb.14.1.50.
Xue-Franzén Y, Kjærulff S, Holmberg C, Wright A, Nielsen O. 2006. Genomewide identification of pheromone-targeted transcription in fission yeast. BMC Genomics. 7:18.doi:10.1186/1471-2164-7-303.
Yazawa H, Ogiso M, Kumagai H, Uemura H. 2014. Suppression of ricinoleic acid toxicity by ptl2 overexpression in fission yeast *Schizosaccharomyces pombe*. Appl Microbiol Biotechnol. 98: 9325–9337. doi:10.1007/s00253-014-6006-y.

Communicating editor: C. Landry